Comp. & Maths. with Appls. Vol. 12B, Nos. 1/2, pp. 329–361, 1986
Printed in Great Britain.

0886–9561/86 $3.00 + .00

MOIRÉS

HANS GIGER
Bueglenstrasse 67, 3006 Berne, Switzerland

Abstract—Moiré phenomenon with its applications is presented and its global geometric properties are analysed and established.

1. INTRODUCTION

Moiré originally was a fabric design with a variable play of lustre. The name is derived from the French word for "watered". The Moiré-technique, discovered and developed in China, was introduced into France in 1754 by the English manufacturer Badger (or Badjer).

Natural or true Moiré is produced by two fabrics which are pressed one onto the other with their ribbed sides or by one fabric which on top of its ribbed side is ribbed by a barrel. False Moiré is a design impressed on a smooth fabric.

One of the first to investigate the Moiré phenomenon was Lord Raleigh (1845–1919), the wellknown English physicist. The Moiré phenomenon is based on purely geometric principles and its scientific applications are therefore rather rare. Moirés are used as analog computers, as models of physical patterns and they are applied to optics and to the investigation of perception.

The sense of aesthetic delight derives from the fact, that the Moiré phenomenon produces order out of unobserved order or even order out of chaos. This property also seems to be its mathematical content because, to some extent, the whole object of mathematics is to create order where previously chaos seemed to reign, to extract structure and invariance out of the midst of disarray and turmoil, or in one word, to establish symmetry.

Furthermore this property of the Moiré phenomenon shows an amazing relationship to our senses: a Moiré is an undifferential, global Gestalt phenomenon which to some extent depends on the corresponding properties of the eye. In this article, the Moiré phenomenon with its applications is presented and its global geometric properties are analysed and established.

2. THE MATHEMATICAL MOIRÉ

Moiré patterns occur quite often in daily life. If we observe the folds of a slightly moving nylon curtain with small mesh we can see these patterns moving about.

Figure 1 is the photograph of a Moiré-silk. The special treatment gives the fabric a design which resembles the surface of water, hence the name.

Figure 2 shows two different ways of producing Moiré-patterns. In Fig. 2(a) the two black and white components of textures are geometrically superposed by forming the union of the two pointsets. In Fig. 2(b) the components of Fig. 2(a) are overlaid in the sense of geometric intersection, i.e. the white elements may be interpreted as apertures in the black areas of the two components. Obviously, the components in Fig. 2(a) and 2(b) are themselves Moirés in the sense of the described superposition. Such patterns are used as models of random point sets (colloids with gel structure, liquids, mineralogic deposits) and their mathematical properties are known to a great extent.

Often the texture components are systems of black lines or opaque screens with holes arranged along the u- and v-curves of a general mathematical net of coordinates. In each point (u, v) of the net, an u- and a v-curve intersect. Any algebraic relation between u and v, such as $u + v = k$ or $u - v = l$, where k and l are integers, defines a curve of the Moiré.

In Fig. 3 the points with a constant sum or difference of their coordinates are linked by a pointrow. If k or l runs over some subset of the integers, a set of Moiré curves is defined. They produce the Moiré-texture of the corresponding algebraic relation. The freedom in the choice of the algebraic relation brings discretion into the concept of Moiré-texture but makes it convenient

Fig. 1.

for mathematical investigations[1]. A more synthetic interpretation of Moiré-textures will be given in Sec. 4.4.

3. PSYCHOLOGICAL MOIRÉS

The arbitrariness in the mathematical concept of Moiré given in the last Section becomes obvious, if the laws of seeing are taken into account. The human eye, on its lowest levels of image processing, is ordering points according to their neighbourhood. In each quadrangle of Fig. 3 the smaller diagonals seem to be emphasized as shown in Fig. 4 and therefore the discussed algebraic relation $u - v = l$ stands informationally out.

Generally human perception seems to extract order out of static or dynamic disorder or impresses order on chaos by investigating or creating correlations between the percepted ele-

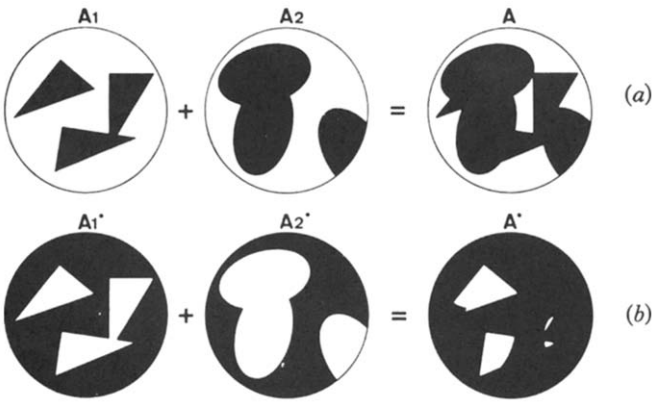

Fig. 2.

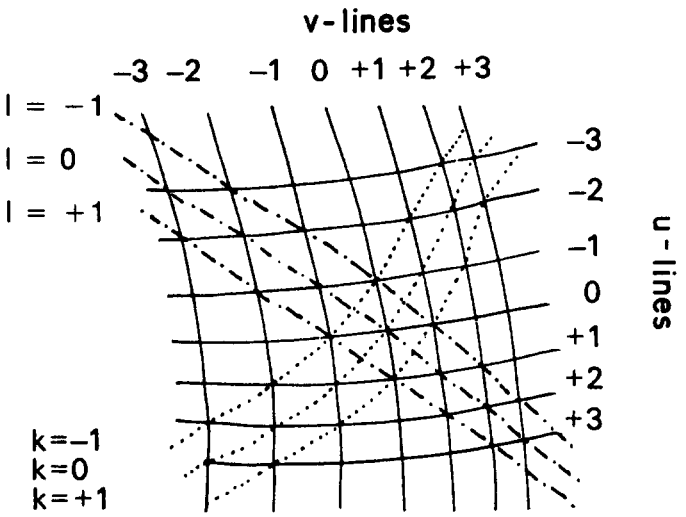

Fig. 3.

ments. In a general sense, these faculties of the eye seem to correspond to the capacities of the ear, which is capable of extracting overtones from a tone.

Figure 5 shows the superposition of two identical random-dot fields after Klein[2]. The copy is first covered by the original field and the latter is then turned by a small angle around a fixed point relative to the copy. The eye sees a Moiré-texture of concentric circles. Similar effects of ordering after MacKay[2] occur in dynamic processes. If a white random noise produced on a television screen is looked at through a fine ruling, a radial order is observed.

Observing Moiré-textures we often see physiological colors, as they appear on a rotating Benham disk (Fig. 6). The ever moving Moiré-fringes, transformations caused by the movement of the object or the observer, can be answered by the eye with the complement of the transformation. If we fix the moving surface of a river for a certain time and then suddenly look at the bank we see it moving river upwards. This effect can be the cause of uncertainty or even dizziness.

4. SCIENTIFIC APPLICATIONS

Moiré textures have different scientific applications, the most important of which will be described in this section.

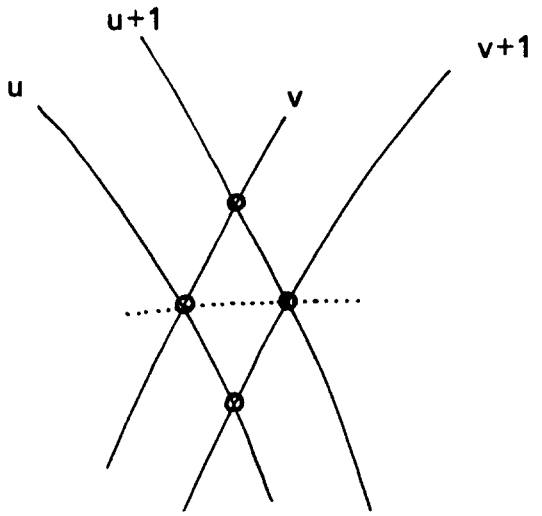

Fig. 4.

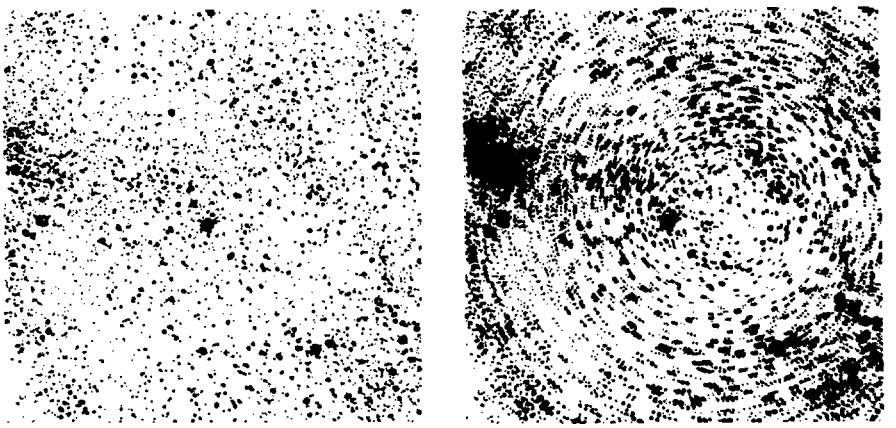

Fig. 5.

4.1 *Lensless enlargement*

Printers often have problems with Moiré-patterns formed by two superposed screens which are not correctly combined. Figure 7(a) shows such a superposition. In the resulting pattern the constituting identical figures (e.g. squares, hexagons) of the screens emerges in an enlargement depending on the relative position of the superposed components. In Fig. 7(b) the superposition of the two rulings results in the same effect. It can easily be observed if two identical small tooth combs are superposed. Lord Raleigh proposed this effect in 1874 for the control of optical grids. The time analogy of the enlargement effect can be produced by a stroboscope. In film the speed of wheels is slowed down or even turned back by this effect. The enlargement effect of Moirés was used by V. F. Holland in about 1960 to make the arrangement of the particles in a crystal visible. W. H. Bragg and W. L. Bragg used this effect in 1915 by superposing several X-ray diffraction pictures to reconstruct the molecule hexamethylbenzol.

4.2. *Correlations in random textures*

If two black and white textures are superposed on each other or on a ruling, relations in the texture can be made visible by the Moiré-effect. Figure 8 shows an anisotropic texture. If a ruling is superposed in different directions the restorder in the texture can be demonstrated.

The Moiré effect can be used to demonstrate the hidden periodicity in the following texture: If a handfull of pebbles is arranged in a row so that two successive pebbles are in contact, this

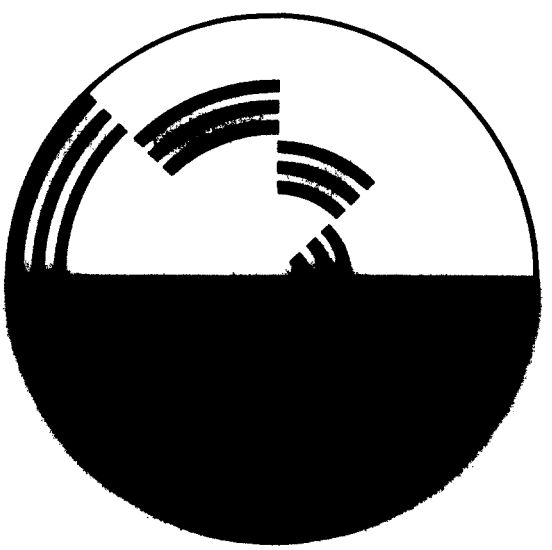

Fig. 6.

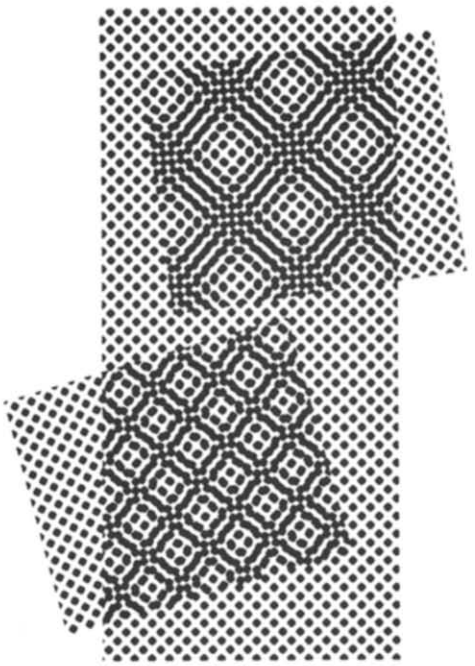

a

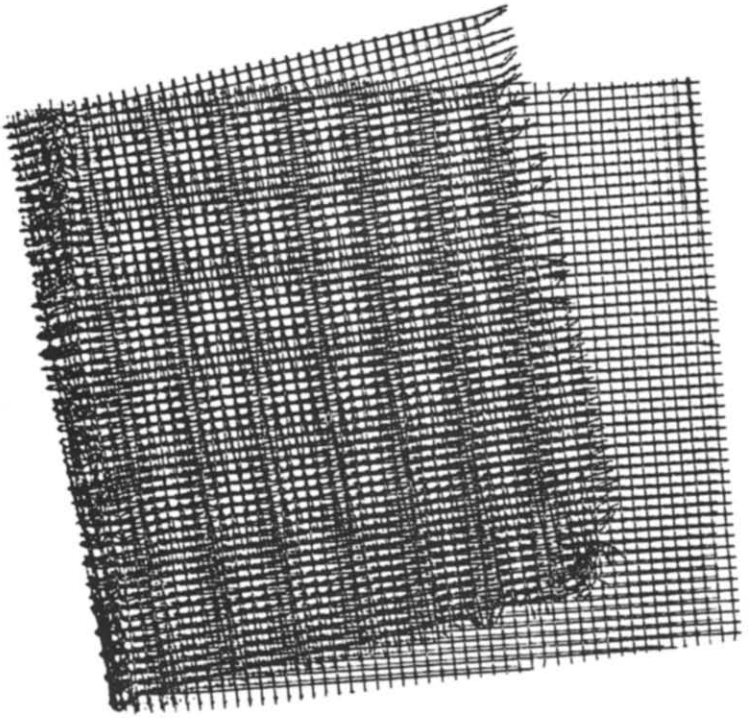

b

Fig. 7.

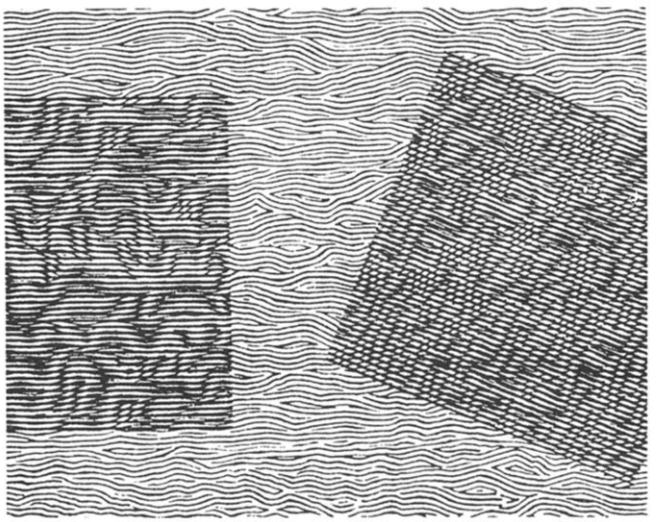

Fig. 8.

chain has an inner periodicity the period of which equals the mean length of the pebbles in the direction of the row. In Fig. 9 this pattern of pebbles is represented by vertical lines with varying spacings. The variation of the spacing is a certain percentage, say 20%, of the mean distance between the lines. The obtained ruling is now inclined at a certain angle so that the lines of the first and second ruling intersect on a horizontal line. In the resulting Moiré-pattern the hidden periodicity of the random texture appears in the horizontal Moiré fringes which get more and more disturbed if the distance from the intersection line grows[3].

4.3 *Pattern simulation*

Moirés can be used to simulate different patterns. This can be shown by two examples. Figure 10 shows the correct representation of the electric field in a plane through an electron and a proton. In a similar way the streamlines in a plane of a streaming liquid can be simulated. Figure 11 is the simulation of the interfering waterwaves occuring when the surface of a pond is excited simultaneously at two different points.

4.4 *Representation of planes curves and surfaces*

With a plotter governed by a computer, a plane curve can approximately be represented as a point-row, the points of which are often linked by straight segments, or as an envelope to

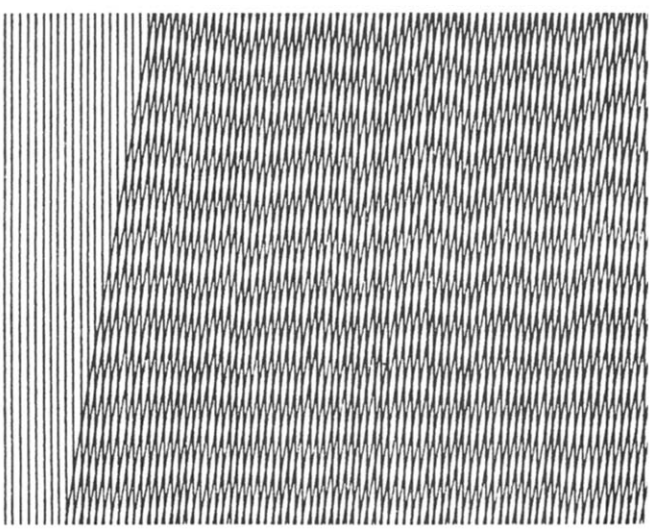

Fig. 9.

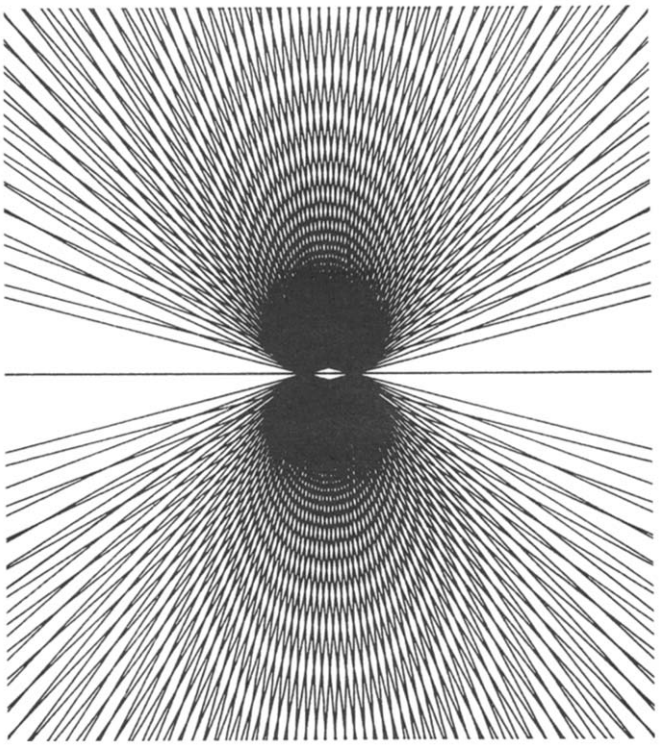

Fig. 10.

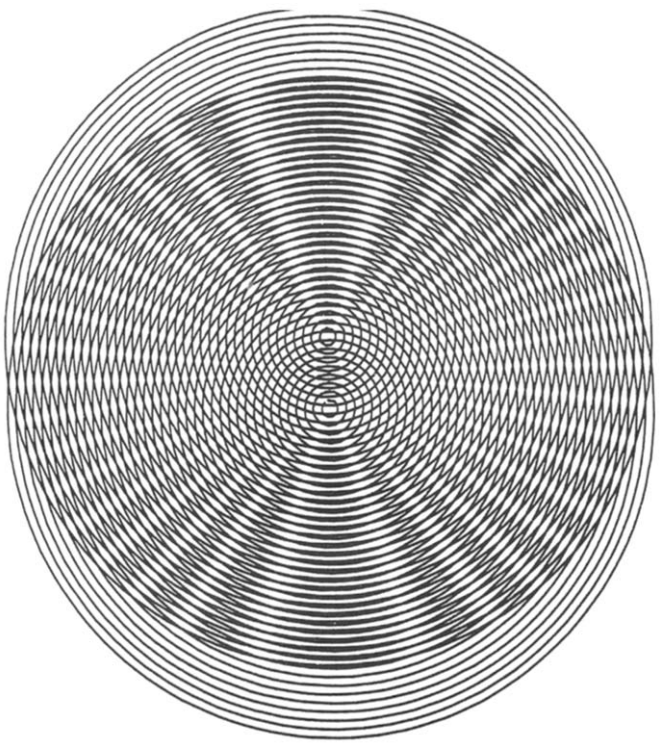

Fig. 11.

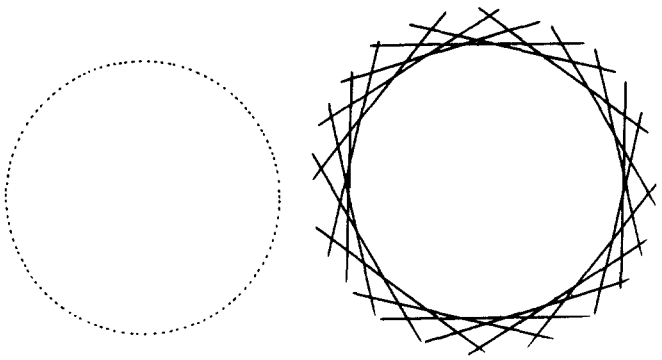

Fig. 12.

the curve (Fig. 12). Less known is the possibility of representing the graph of a function of one or two variables by a Moiré-pattern. A possibly new method will be described in this section. Because this construction may be of broader interest, technical details are omitted and will be given in Appendix 1.

We restrict the concept of Moiré to the superposition of two linefields L_1 and L_2. The resulting Moiré $L_1 \cup L_2$ can be understood on the basis of two theorems which are the consequence of interpreting the middle lines of the Moiré-fringes as a selection of the contours of the graph of a function of two variables $z = z(x, y)$ in exactly the same way as contours of a geographical map convey information about the height of the land. Figure 13 gives the contours of a landscape. The contours in the surrounding of a point are the straight evenly spaced contours of the tangent plane of the land. Figure 14 shows the contours of a selection of functions $z = z(x, y)$.

It is also possible that the contours of $z = z(x, y)$ are radial fields of lines, Fig. 15(a). Two examples are given in Fig. 15(b, c). One of the graphs can be described by $z = \varphi$, the other by $z = \ln [\text{abs}(\tan (\varphi/2))]$, if the parameter φ is the angle of the polar coordinates in the x-y-plane.

The question arises: which fields of lines L_1, L_2 have to be chosen to obtain a certain contour Moiré $L_1 \cup L_2$, the fringes of which are the contours of the graph of a given function $z = z(x, y)$. Pairs of linefields L_1 and L_2 which give rise to the same Moiré will be termed *moiré-equivalent*. The answer to the question is given by the following construction that can be generalized (Appendix 1).

Figure 16 shows the graphs of two different functions $z_1 = z_1(x, y)$ and $z_2 = z_2(x, y)$. If these graphs are cut by parallel equidistant planes the projection of the lines of intersection onto the x-y-plane produces linefields L_1 and L_2. In the limiting case H the linefields are the projections

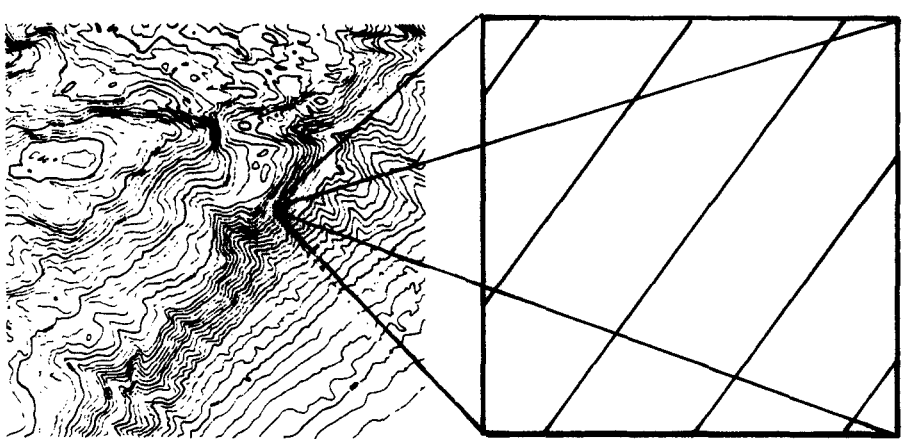

Fig. 13.

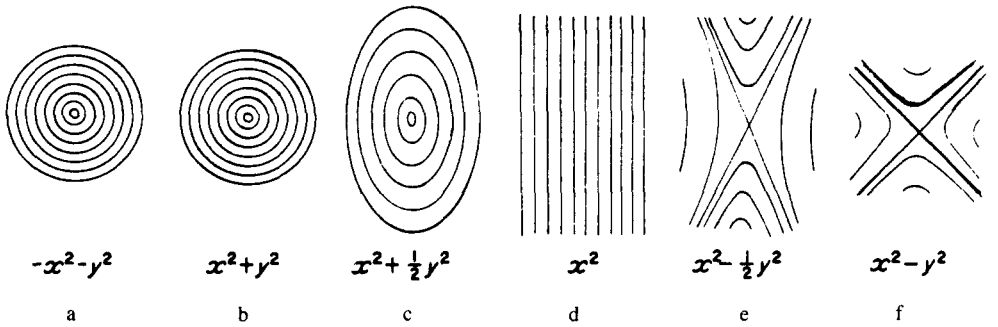

Fig. 14.

of the contours of the graphs of z_1 and z_2. In the other limiting case G the intersection lines on the graphs project in the same ruling on the x-y-plane. The case G is to be excluded.

The first statement is given by

THEOREM 1

The Moiré $L_1 \cup L_2$ does not depend on the direction and inclination of the cutting planes. This fact raises the question in what way the Moiré $L_1 \cup L_2$ depends on z_1 and z_2. In the limiting case H the answer can be given: If z_1 is a horizontal plane, $z_1 =$ constant, L_1 is void. Therefore $L_1 \cup L_2 = L_2$ is the contourmap of the graph of z_2 with equidistance determined by the horizontal cutting planes.

With Theorem 1 we obtain

COROLLARY

If z_1 is a horizontal plane the Moiré $L_1 \cup L_2$ is the contourmap of the graph of z_2 for each system of cutting planes.

In the general case the preceding question is answered by

THEOREM 2

The Moiré $L_1 \cup L_2$ is the contourmap of $z = z_2 - z_1$.

The well-known indefiniteness of a geographical map, where the contours of a hill can be interpreted as the contours of a pit and vice versa, must also be taken into consideration with Moirés; i.e. z can also be described by $z = z_1 - z_2$. The graph of the difference function z is represented by Fig. 17. The vertical rods between z_1 and z_2 must be lowered till the deeper ends meet the x-y-plane.

A consequence of Theorem 2 indicated by Fig. 18 is of special interest. The Moiré works as analog computer and differential analyzer. Beside the superposition of two different linefields L_1, L_2, it is also possible to overlay two identical fields $L = L_1 = L_2$ of $z = z_1 = z_2$ in translating or rotating one of the fields relative to the other or in superposing the stretched field λL with L. Translation is denoted by L^τ, rotation by L^φ.

The effect of selfsuperposition is described by

THEOREM 3

The Moiré $L_1 \cup L_2$ with $L = L_1 = L_2$ in the case of

- a small translation is the contourmap of the partial derivative of z in the given direction of the translation;
- a small rotation is the contourmap of the rotational derivative of z;
- small stretching is the contourmap of the radial derivative of z.

The word "small" in the theorem is used in the sense of calculus. A strict formulation has to take into account that in order to get a contourmap with fixed equidistance the distance between the cutting planes has to be taken infinitesimal if the transposition nears identity. Demonstrations of the three theorems are given by the following figures.

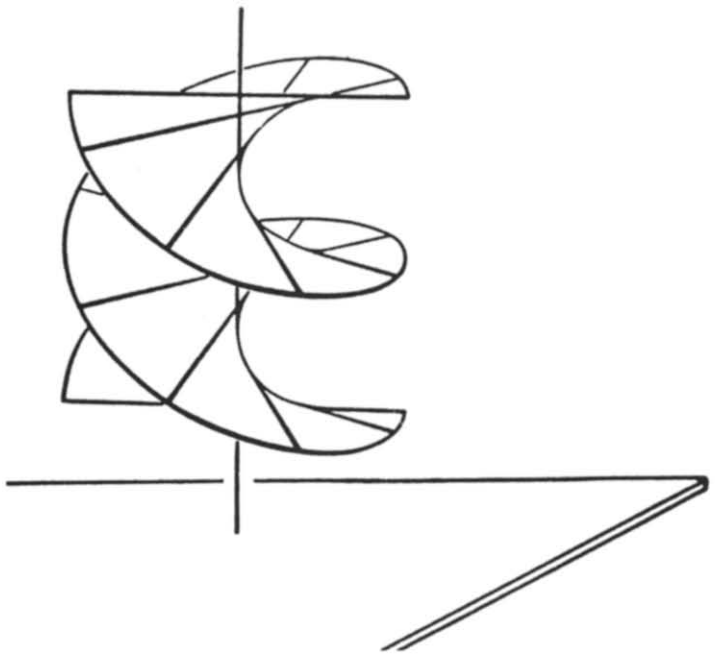

a

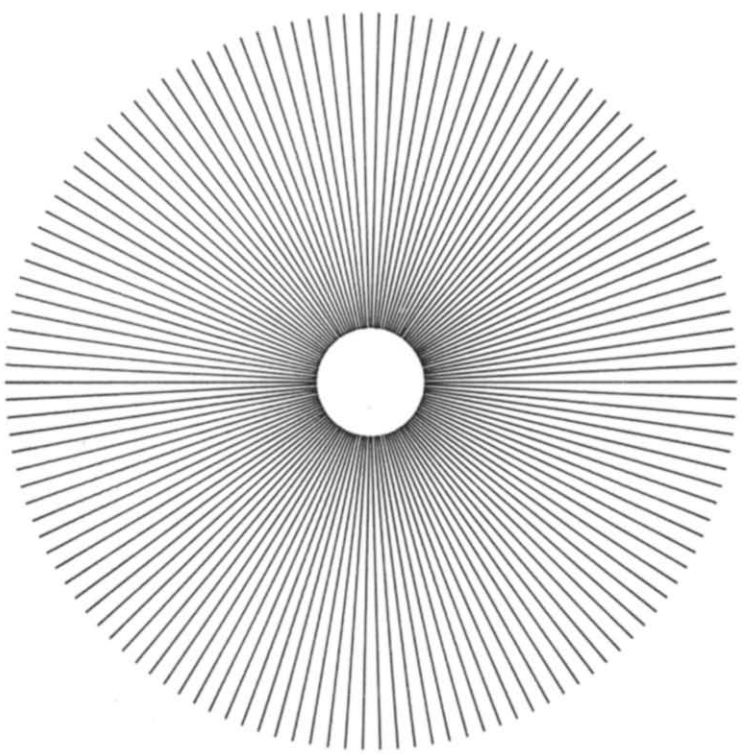

b

Fig. 15(a–c).

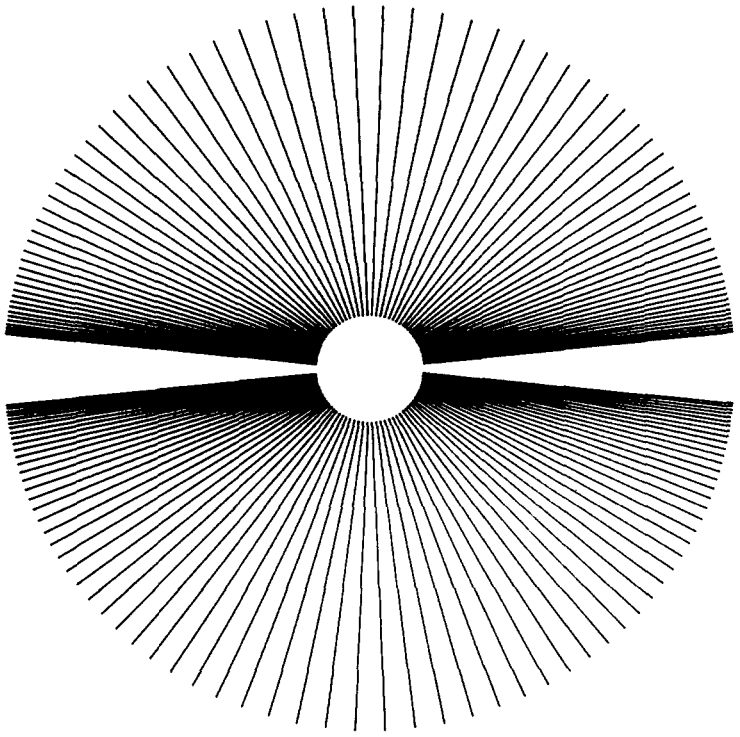

c

Fig. 15. (*Con't*)

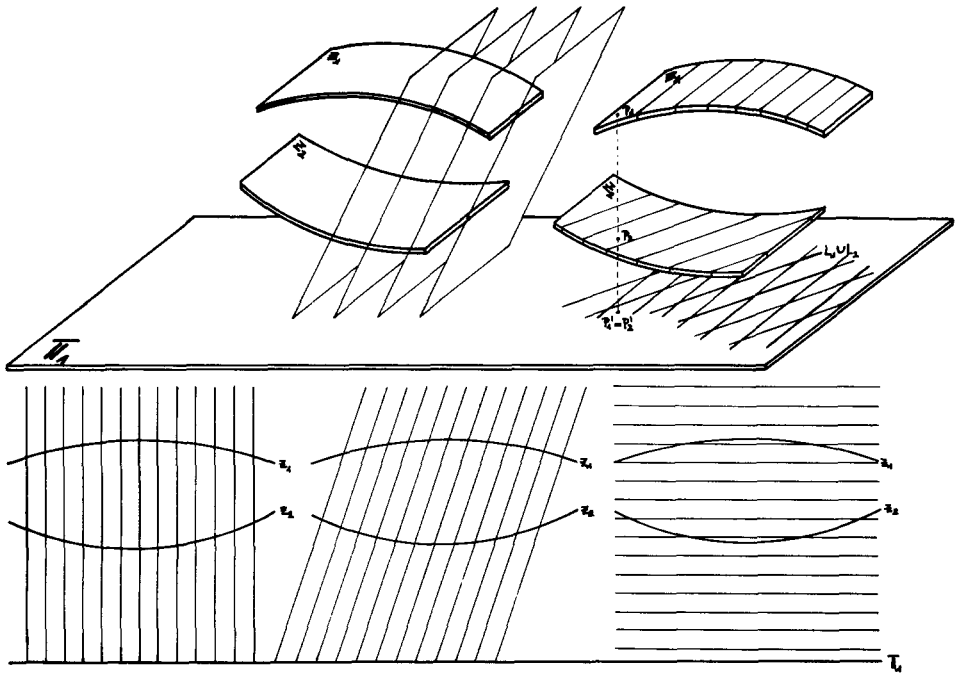

Limiting Case G **Limiting Case H**

Fig. 16.

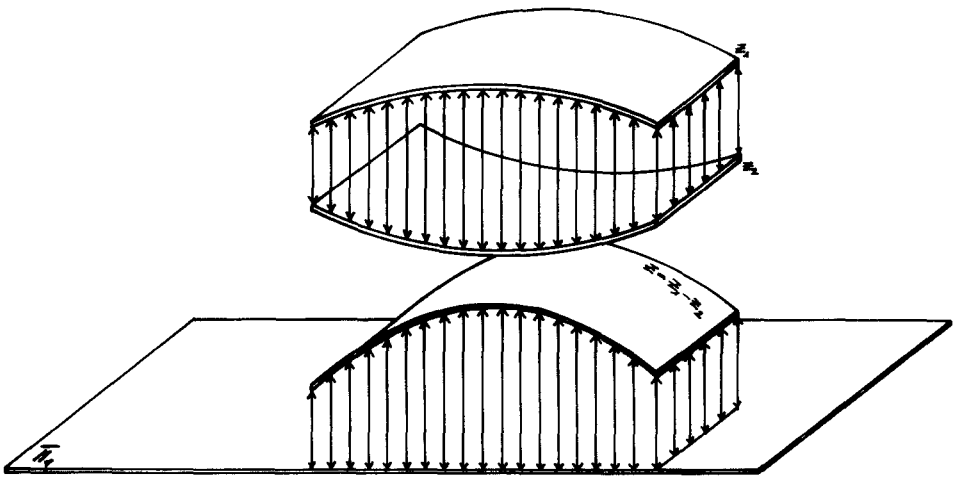

Fig. 17.

Figure 19(a) explains the formula used in the Appendix 1 that relates the spacings a and b of the two superposed rulings and the angle φ between a straight line of the first and one of the second ruling to the distance d between adjacent Moiré-fringes. Figures 19(a) and 19(c) demonstrate the two possibilities of superposing two rulings that, according to Fig. 16, can be interpreted as the intersection lines L_1 and L_2 when two planes given by $z_i = a_i x + b_i y + c_i$, $(i = 1, 2)$, are cut by a system of the equidistant planes. The resulting Moiré is according to Theorem 2 the contourmap of the plane $z = z_1 - z_2$.

Figure 20(a) gives the contour Moiré $L_1 \cup L_2$ of a hill or a pit. L_1 is constructed according to Fig. 16 as the linefield of $z_1 = \hat{x}^2 + \hat{y}^2 + ax + by + c$; L_2 as that of $z_2 = ax + by + c$. The resulting Moiré is the contourmap of the paraboloid $z = z_1 - z_2 = \hat{x}^2 + \hat{y}^2$. Figure 20(b) shows the Moiré of the selftransposition $L \cup L^\tau$, where L is the contourmap of $z = \hat{x}^2 + \hat{y}^2$. The resulting contourmap is, according to Theorem 3, the map of the plane $Dz = 2\alpha x + 2\beta y$, i.e. the directional derivative of z in the direction $\tau = (\alpha, \beta)$, $\hat{\alpha}^2 + \hat{\beta}^2 = 1$. Figure 20(c) gives the superposition of the contourmap $z_1 = \hat{x}^2 + \hat{y}^2$ on a ruling, the contourmap of a plane $z_2 = ax + by + c$. The resulting Moiré seems to contradict Theorem 2. The periodic appearances of systems of concentric Moiré-circles can be explained as a consequence of indefiniteness of the ruling as a map of contours of a plane, because according to the construction of Fig. 16 a set of quantisized planes give the same ruling.

This effect raises the question which linefields L_1 and L_2 should be chosen to get the best

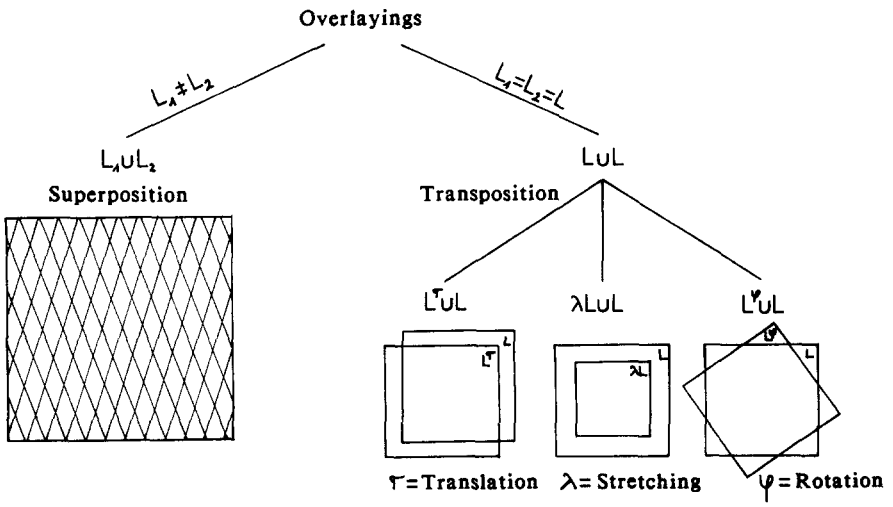

Fig. 18.

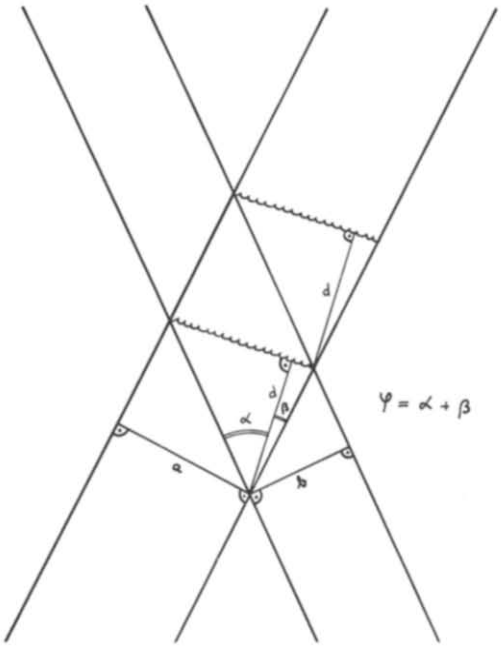

$$d = \frac{a\,b}{\sqrt{a^2 + b^2 - 2ab\cos\varphi}}$$

$\varphi = 0$, $a \neq b$: $d = \dfrac{a\,b}{|a - b|}$

$\varphi \neq 0$, $a = b$: $d = \dfrac{a}{2\sin\frac{\varphi}{2}}$

$$\cos\alpha = \frac{d}{a}\sin\varphi$$

$$\cos\beta = \frac{d}{b}\sin\varphi$$

a

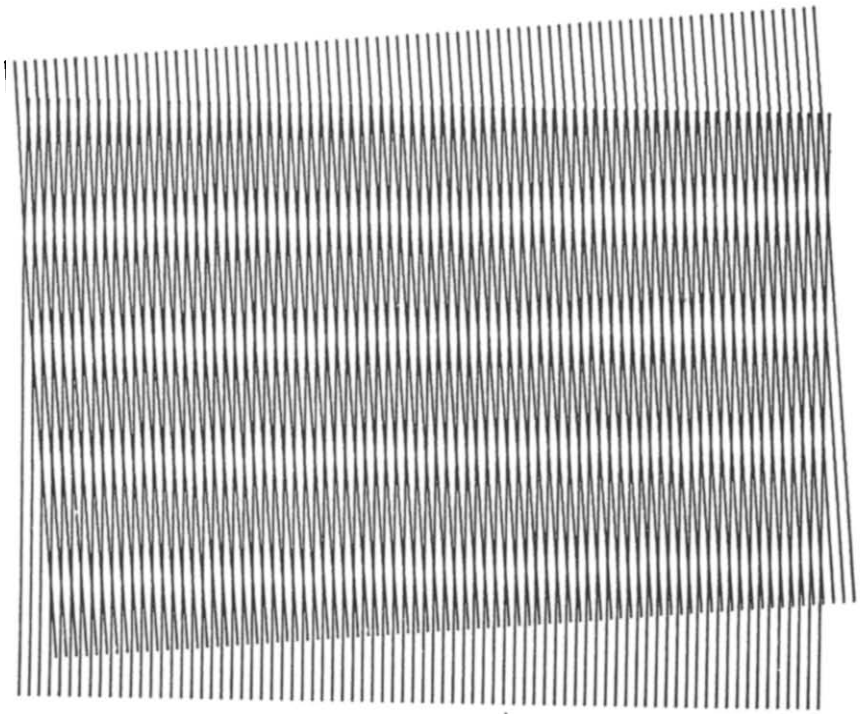

b

$a = b$
$\varphi \neq 0$

Fig. 19(a–c).

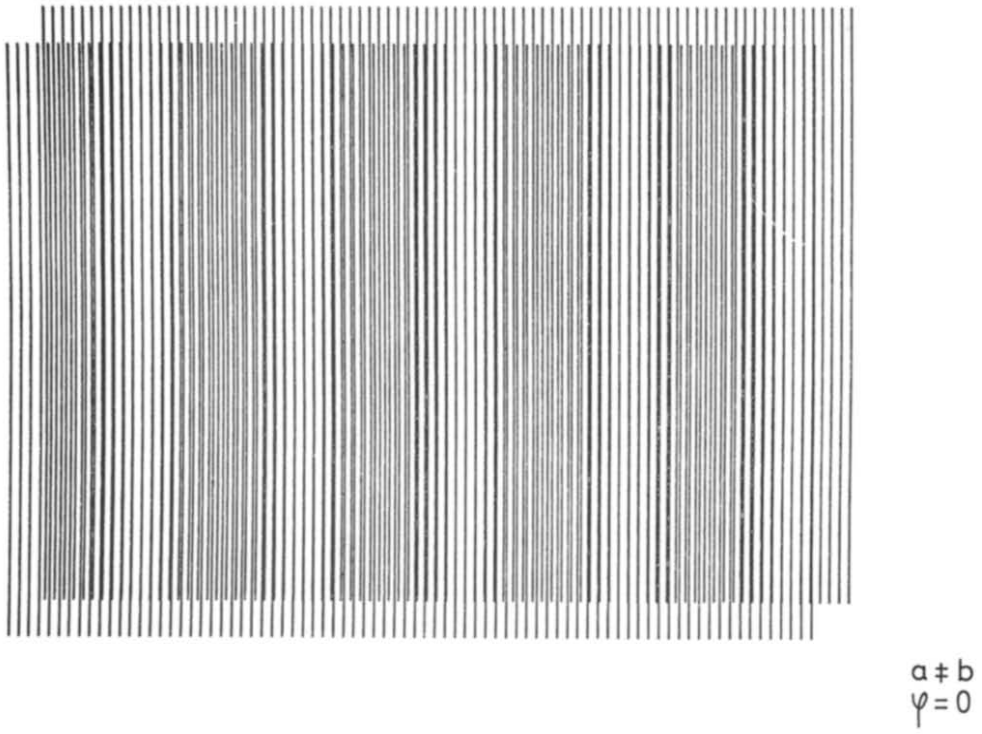

c

Fig. 19. (*Con't*)

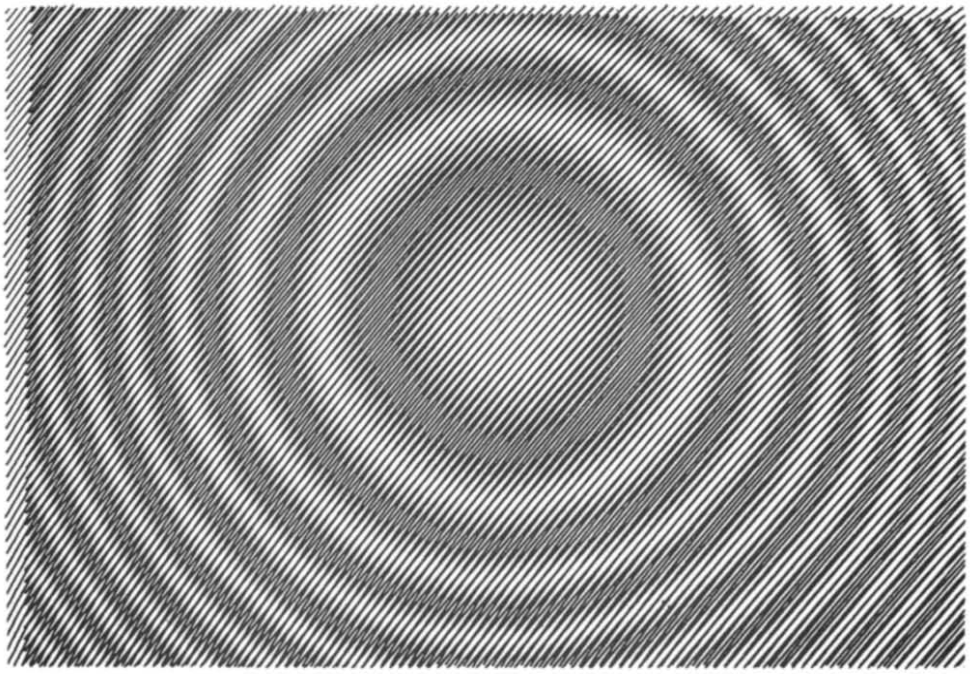

a

Fig. 20(a–c).

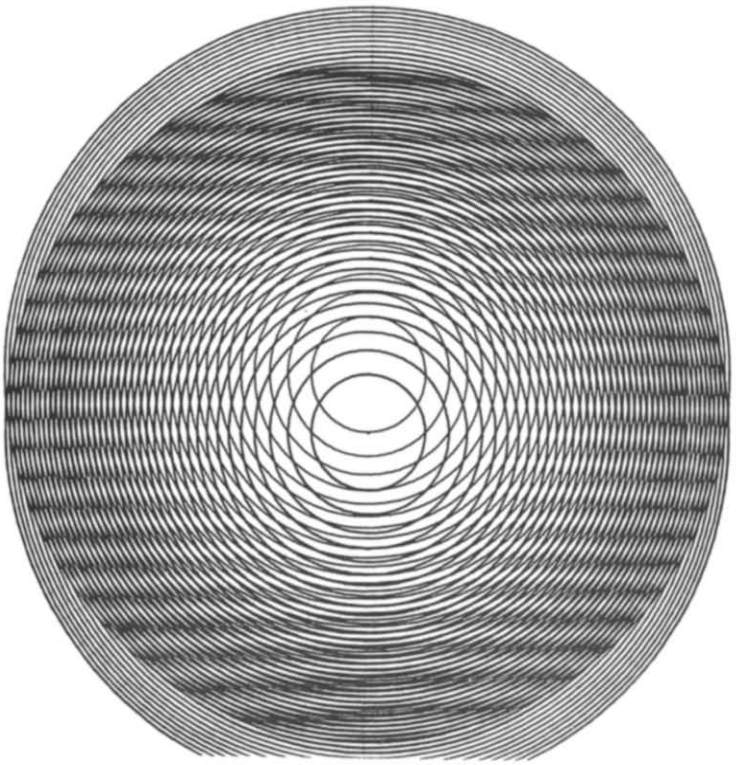

b

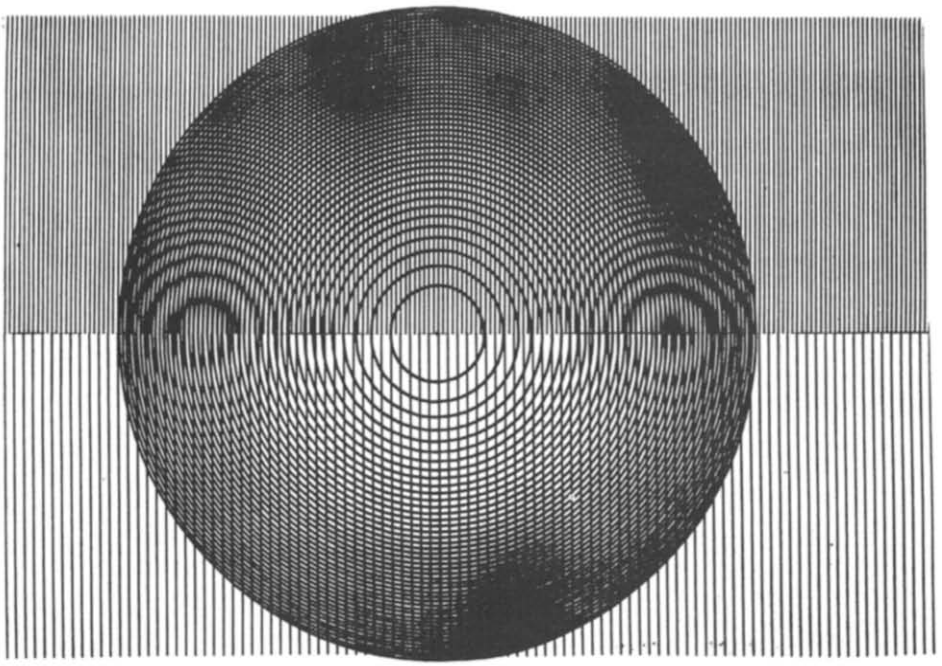

c

Fig. 20. (*Con't*)

representation of a planned contour Moiré $L_1 \cup L_2$. The following answer is substantiated in Appendix 1: The linefields L_1 and L_2 must be constructed such that locally the lines of L_1 and L_2 are nearly parallel to the contours of the desired Moiré.

Figure 21(a) is the contour Moiré of the saddle $z = \hat{x}^2 - \hat{y}^2$ constructed like that of Fig. 20. Figure 21(b) shows the Moiré of the transposition $L \cup L^\tau$, where L is the contourmap of $z = \hat{x}^2 - \hat{y}^2$. As in Fig. 20(b), we obtain the contourmap of $Dz = 2\alpha x - 2\beta y$, the directional derivative of z.

Figure 22(a) is the contour Moiré $L_1 \cup L_2$ of $z = \hat{x}^3 + \hat{y}^3$ constructed like Figure 20(a). Figures 22(b) and 22(c) show two different transportations $L_1 \cup L_1^\tau$, where L_1 is the linefield of $z = \hat{x}^3 + \hat{y}^3 + ax + by + c$. The contour Moiré is the map of the directional derivative $Dz_1 = 3\alpha\hat{x}^2 + 3\beta\hat{y}^2 + k$ and corresponds therefore for appropriate translations $\tau = (\alpha, \beta)$, $\alpha^2 + \beta^2 = 1$, to the maps of Fig. 20(a) and Fig. 21(a). Figures 22(d) and 22(e) give two translations $L \cup L^\tau$, where L is the contourmap of $z = \hat{x}^3 + \hat{y}^3$. The resulting contour Moirés are those of Fig. 22(b) and 22(c). Figure 22(f) is the rotational transposition $L \cup L^\varphi$, where L is the contourmap of $z = \hat{x}^3 + \hat{y}^3$. The origin of the system of coordinates is the fixpoint of the rotation. The contour Moiré is the map of the monkey-saddle $Dz = -3\hat{x}^2y + 3x\hat{y}^2$.

Figure 23(a) gives the correct representation of a function $y = f(x)$, here $f(x) = \exp(-\hat{x}^2/2) + c$. L_1 is the linefield of $z_1 = f(x) - xy$, L_2 those of $z_2 = -xy + y$. (For the reason of this setting see Fig. 23(b). The resulting contour Moiré $L_1 \cup L_2$ is the map of $z = z_1 - z_2 = f(x) - y$ and gives the desired representation. Figure 23(b) gives the transposition $L_1 \cup L_1^\tau$, where L_1 is the linefield of Fig. 23(a) and $\tau = (1, 0)$, a translation in the direction of the x-axis. The resulting Moiré corresponds to $Dz_1 = f'(x) - y$, the derivative of the given function. In the following figures the radial linefields L_1 and L_2 of Fig. 15 are transposed.

Figure 24(a) gives the transposition $L_1 \cup L_1^\tau$, which for $\tau = (0, 1)$ is the Moiré $Dz_1 = \cos\varphi/\rho$ of $z_1 = \varphi$, a system of circles with a common tangent at the origin of coordinates. ρ and φ are the polar coordinates. Figure 24(b) shows the transposition $L_2 \cup L_2^\tau$. For the chosen translation the contour Moiré is a system of concentric circles with centres at the origin of the system of coordinates.

The next figures are concerned with the functions $z_1 = \rho.\ \varphi$ and $z_2 = \rho.\ \exp(\varphi)$ given by polar coordinates ρ, φ [Figure 25(a)]. The contour-maps L_1 and L_2 of these functions are shown in translative, rotative and stretched trans- and superposition according to Fig. 18. Figures 25(b) and 25(c) show $L_1 \cup L_1^\tau$ and $L_2 \cup L_2^\tau$, which as directional derivatives give radial Moiré-fringes.

Figures 26(a) and 26(b) give $L_1 \cup L_1^\varphi$ and $L_2 \cup L_2^\varphi$ the first of which as rotational derivative is a contour Moiré of concentric circles, whereas the second reproduces as contour Moiré the linefield L_2.

Figure 27 demonstrates the superposition $L_1 \cup \lambda L_1$, where λL_1 denotes the stretched linefield L_1, the centre of the stretching lies at the origin. The resulting contour Moiré reproduces the linefield L_1. The same effect is observed with L_2.

Figure 28 represents the two linefields L_1 and L_2 of Fig. 21(a), the superposition of which is the contour Moiré of the saddle $z = \hat{x}^2 - \hat{y}^2$. If this figure is observed with the red–green spectacles used to view stereoscopic pictures, the saddle can be seen as three-dimensional surface. If red and green are interchanged the represented function changes its sign. The stereoscopic effect can also be observed when the two linefields are not combined in the same picture and therefore are not expoundable. This nonrandom pictures like the well-known random dot pictures of Bela Jules can only be interpreted in stereological presentation.

5. SPATIAL MOIRÉS

A spatial Moiré results if two sets of points or lines each of which is located in the three-dimensional space on the graph of one of the functions or relations $z_1 = z_1(x, y)$, $z_2 = z_2(x, y)$ are looked at in diffuse illumination. The objects causing these patterns will also be termed *spatial Moirés*.

If understanding is interpreted in the constructivist sense, that is, a phenomenon is explained if it can be classified, planned and constructed, there is not much insight in the various patterns

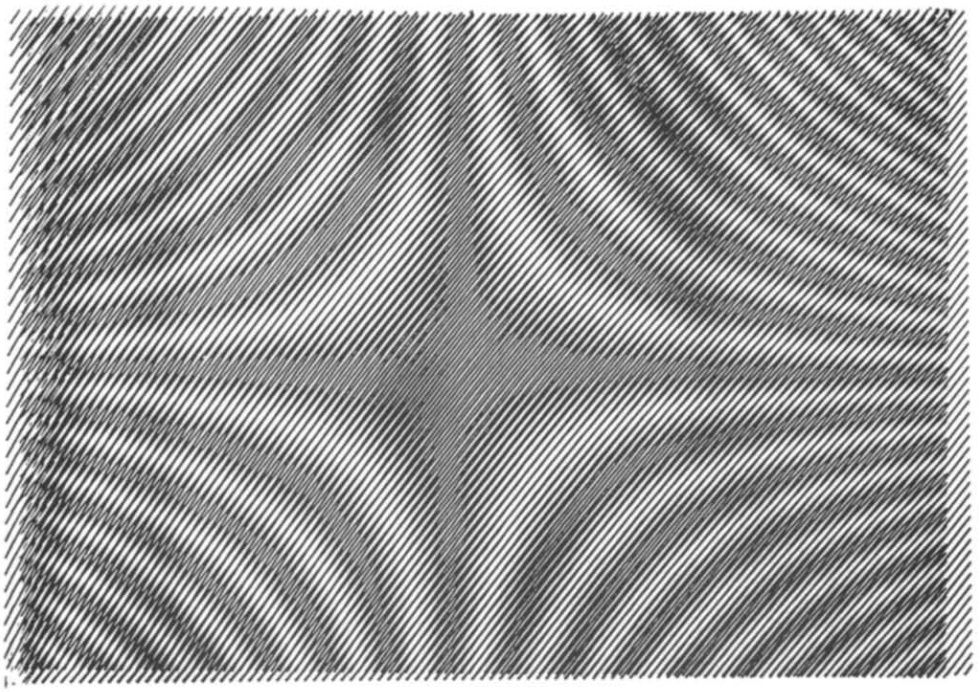

a

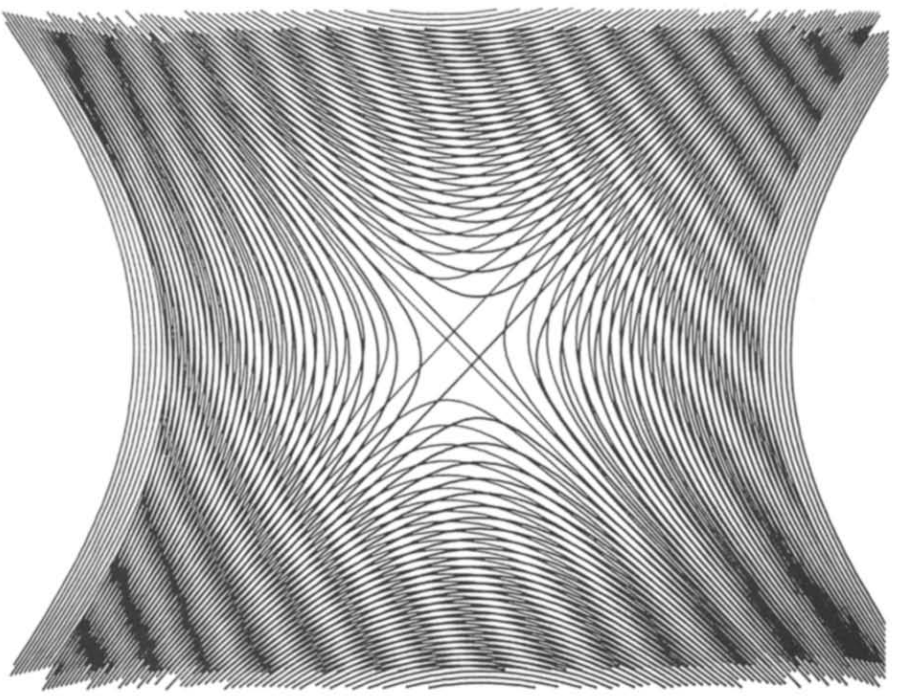

b

Fig. 21(a–b).

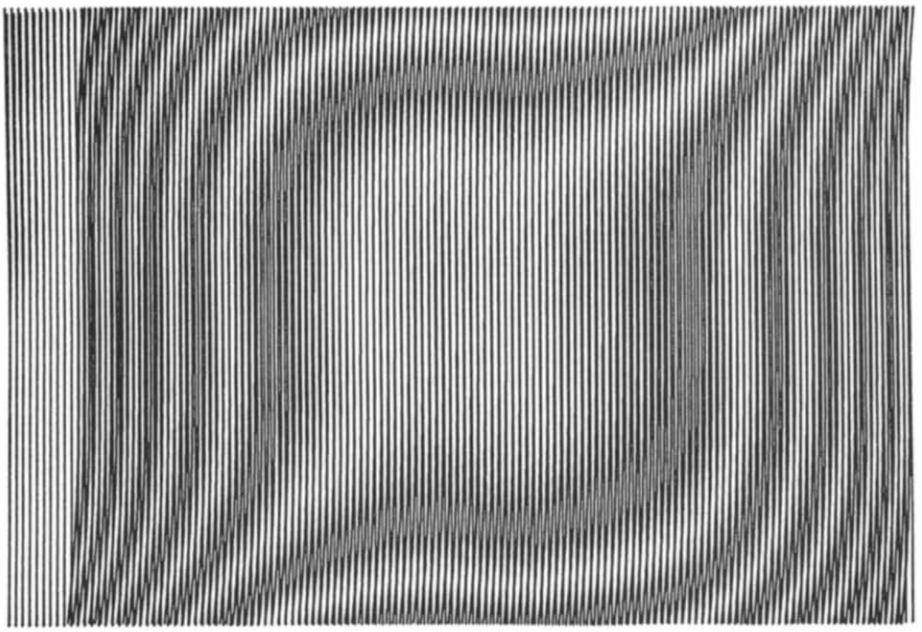

a

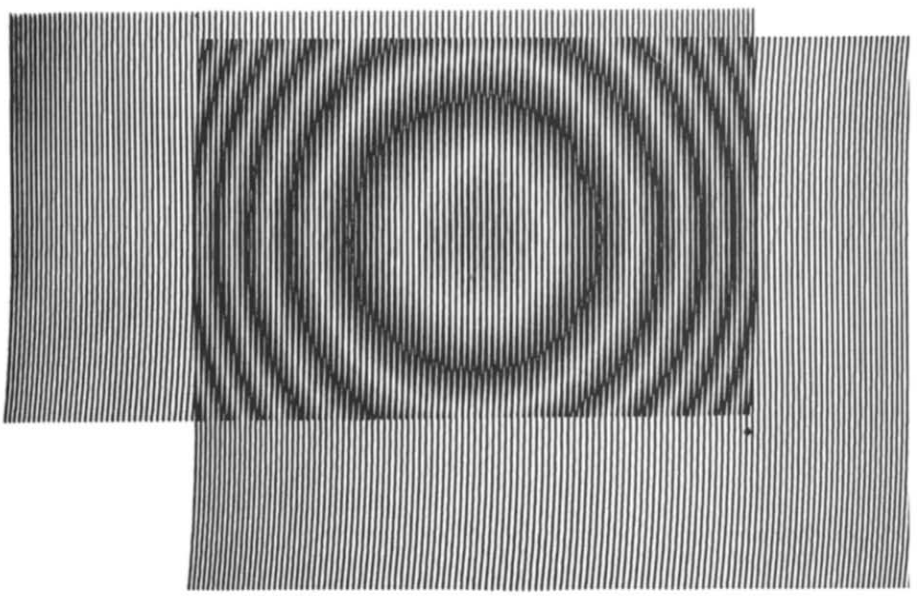

b

Fig. 22(a–f).

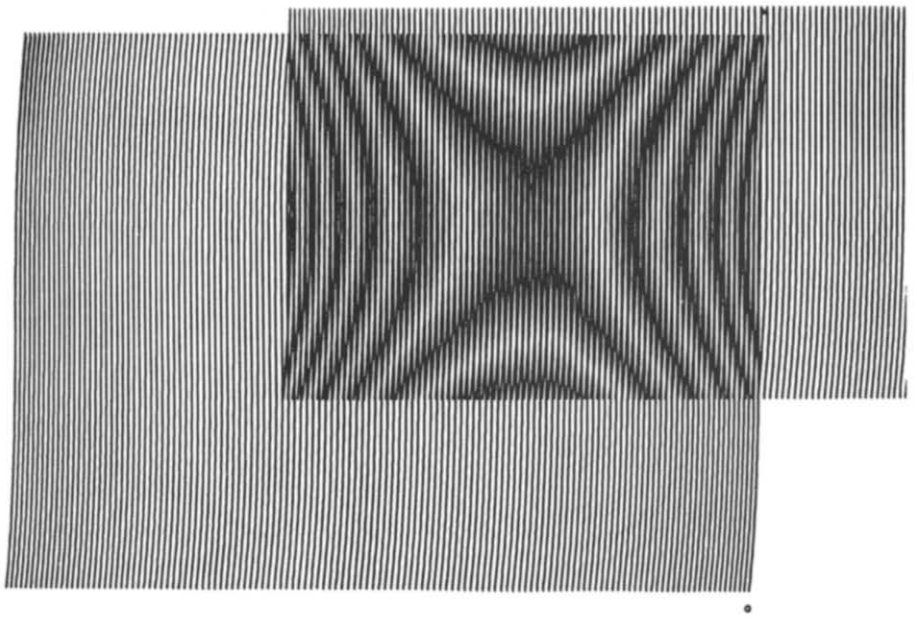

c

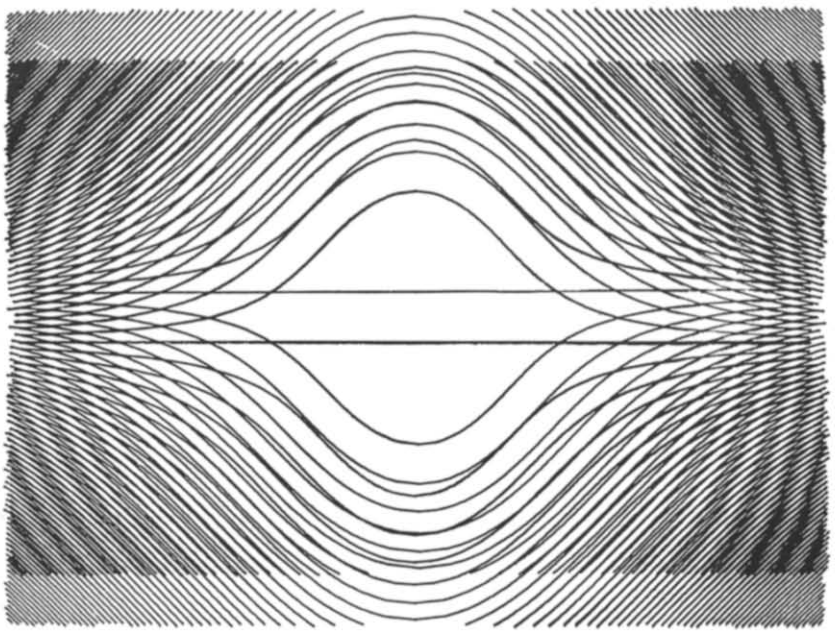

d

Fig. 22. (*Con't*)

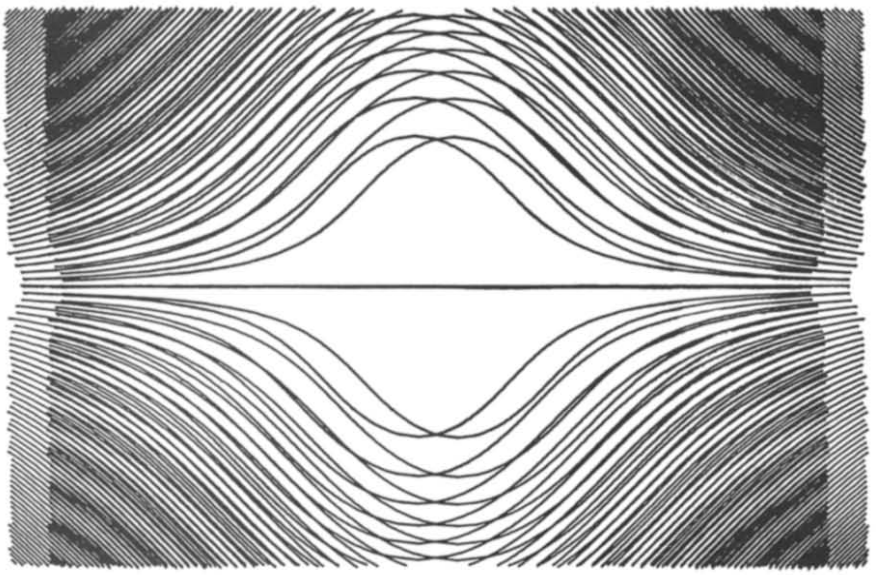

e

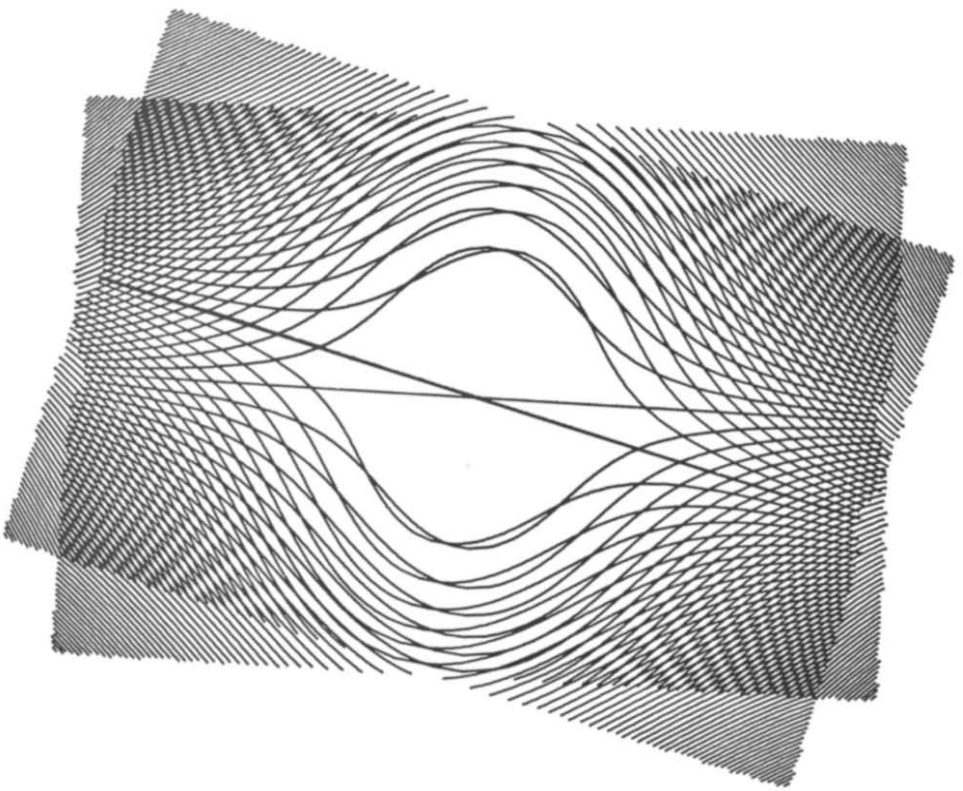

f

Fig. 22. (*Con't*)

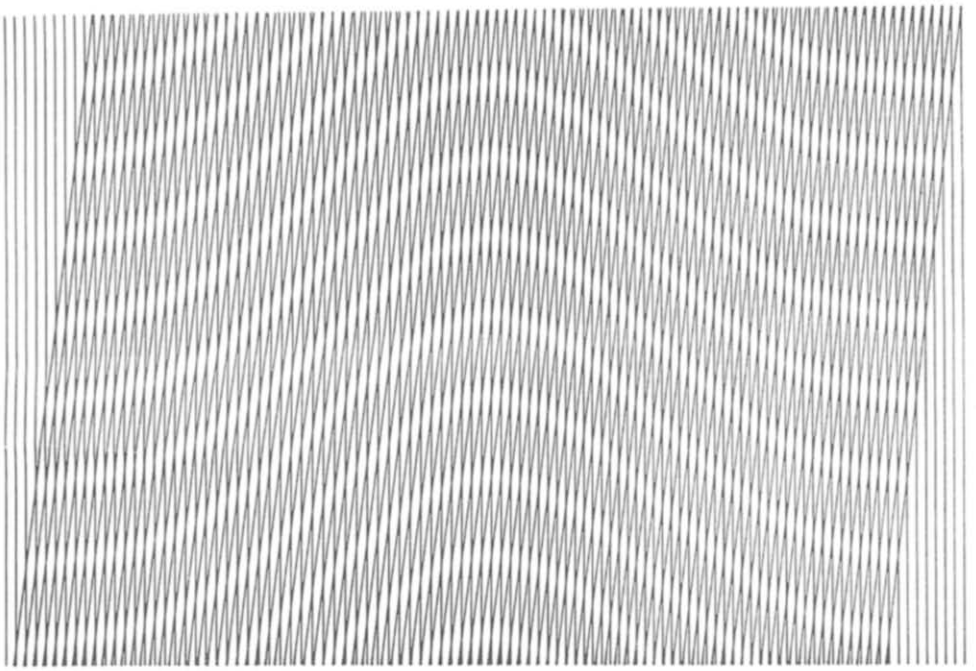

a

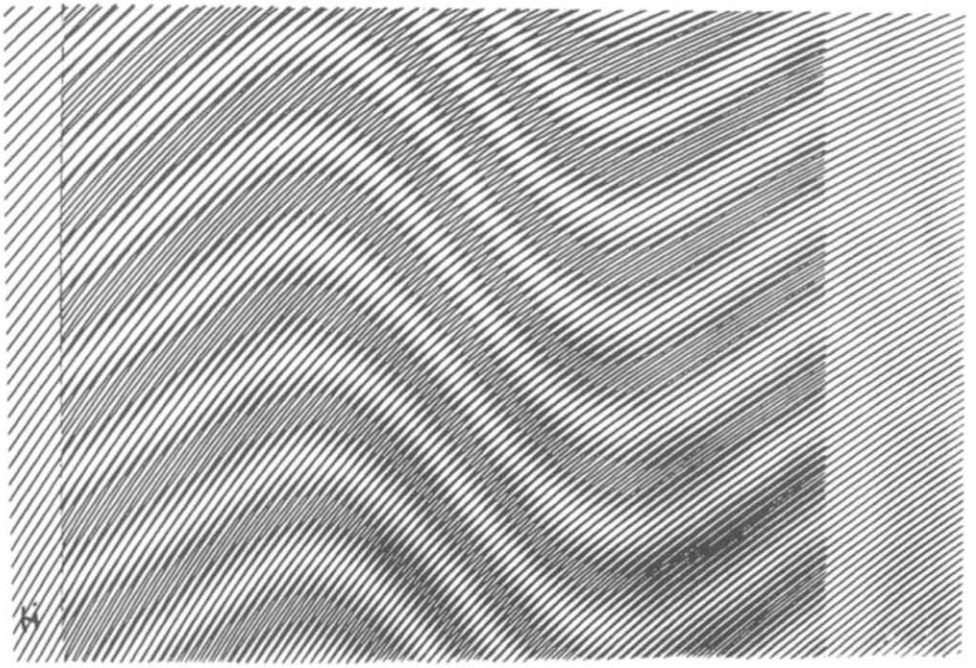

b

Fig. 23.

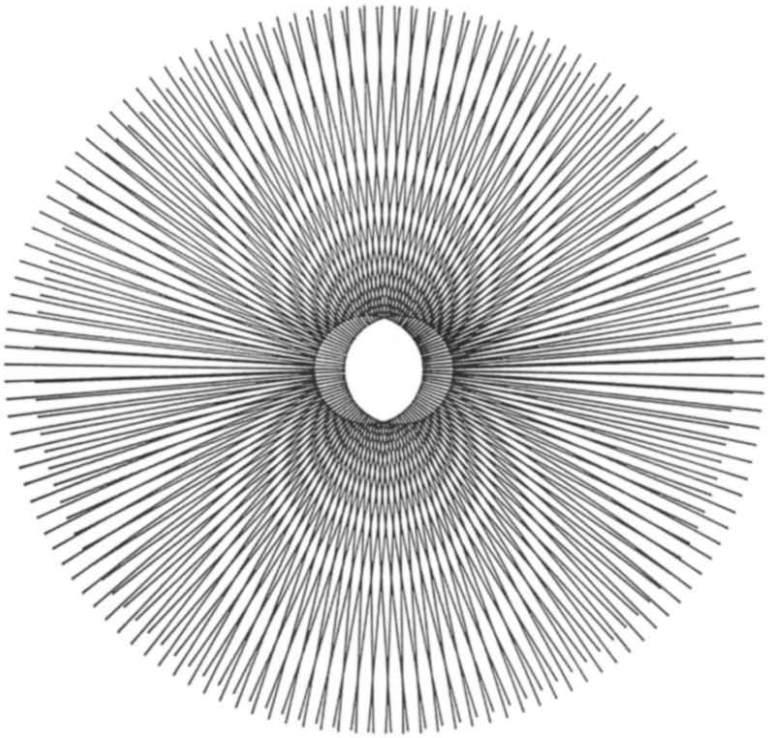

a

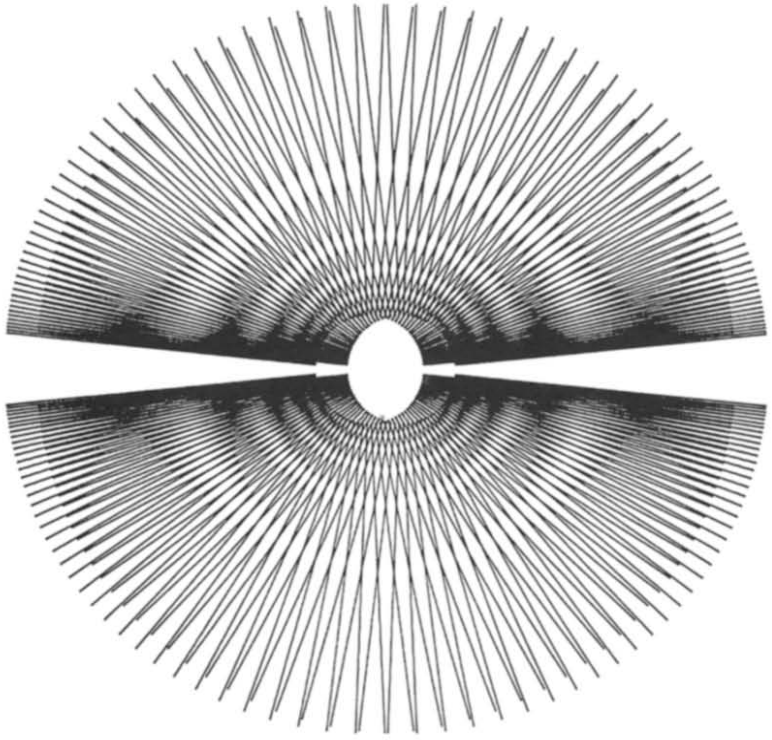

b

Fig. 24.

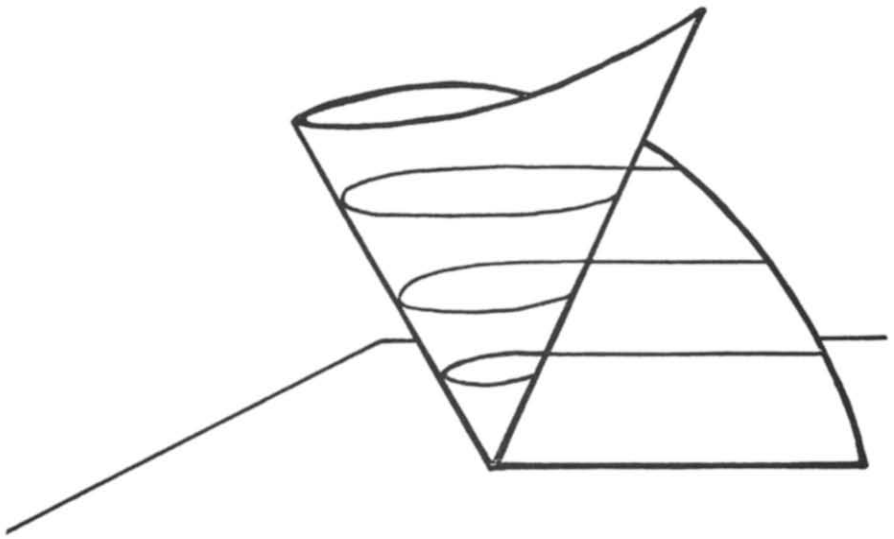

a

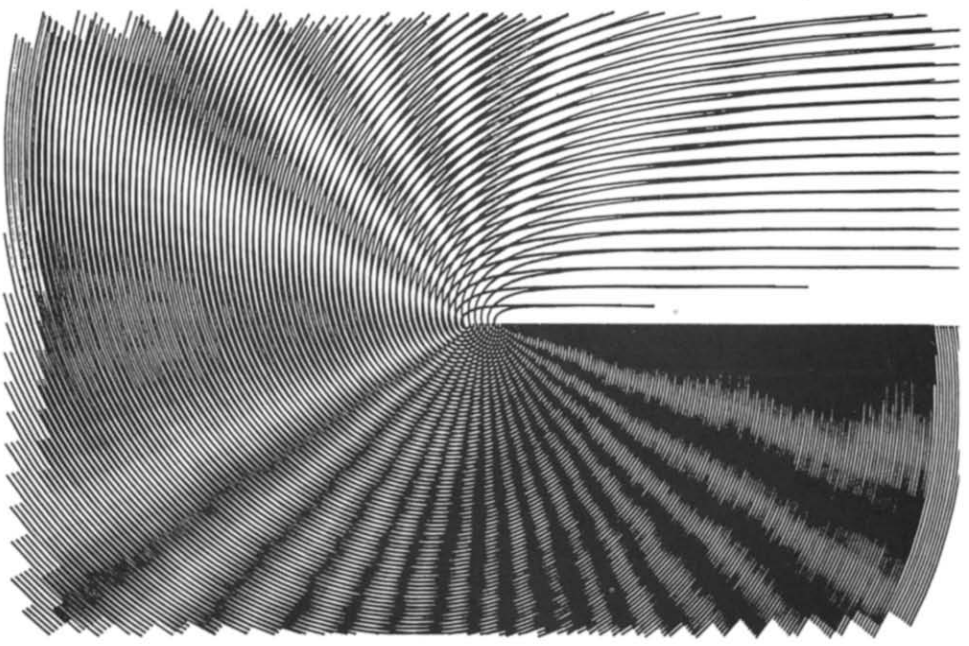

b

Fig. 25(a–c).

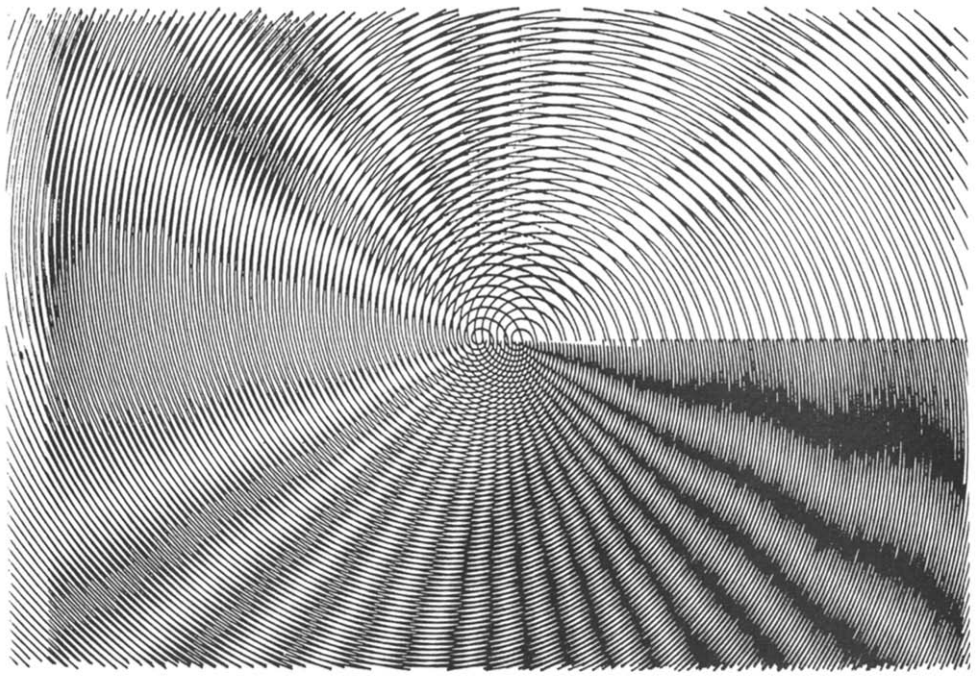

c

Fig. 25. (*Con't*)

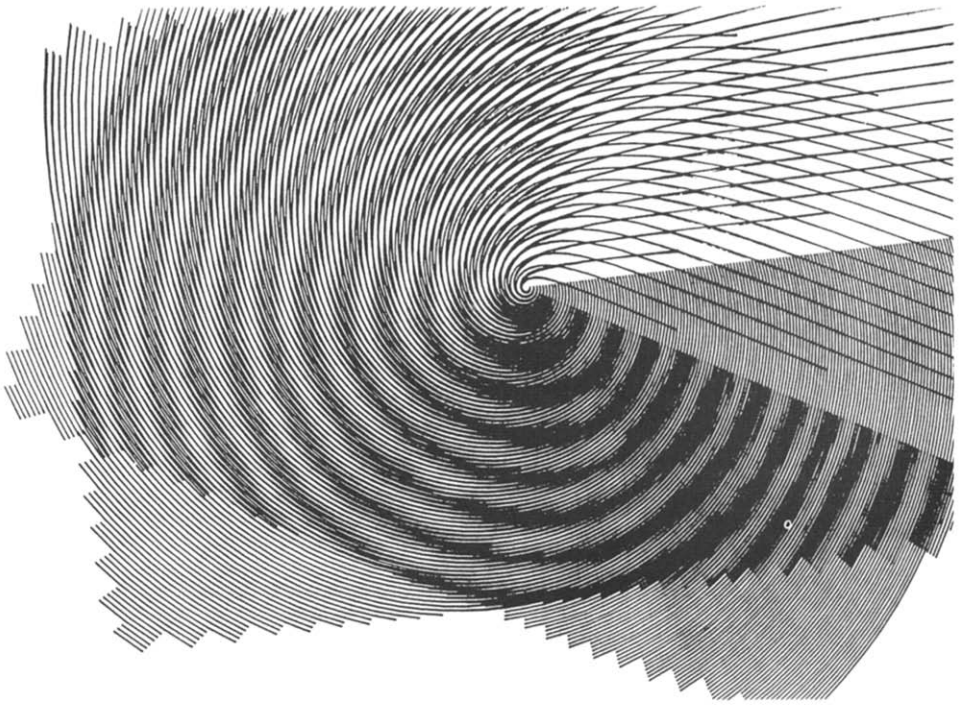

a

Fig. 26(a–b).

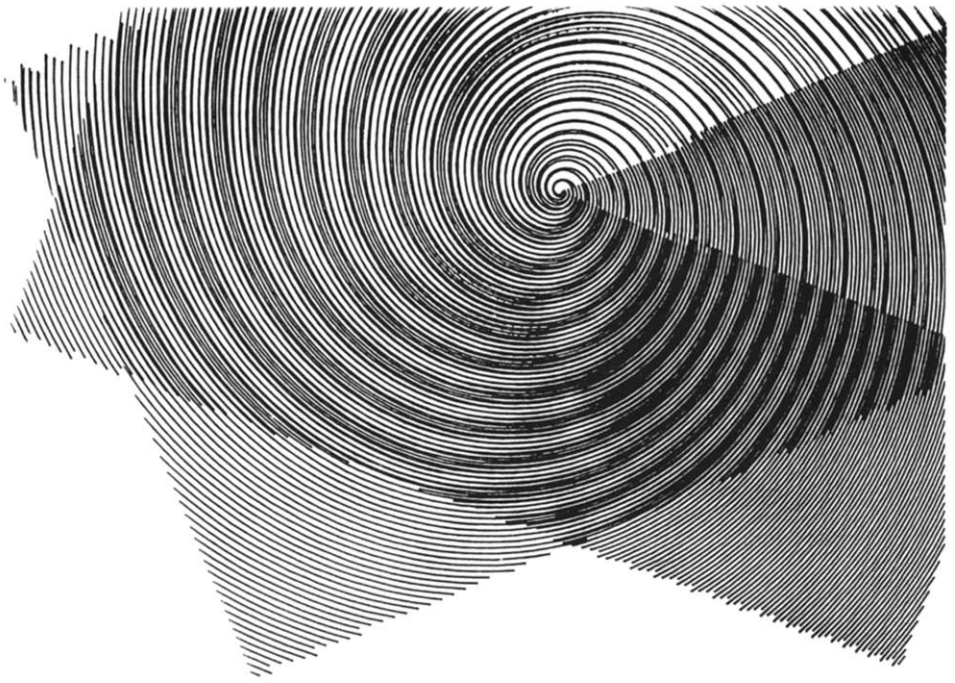

b

Fig. 26. (*Con't*)

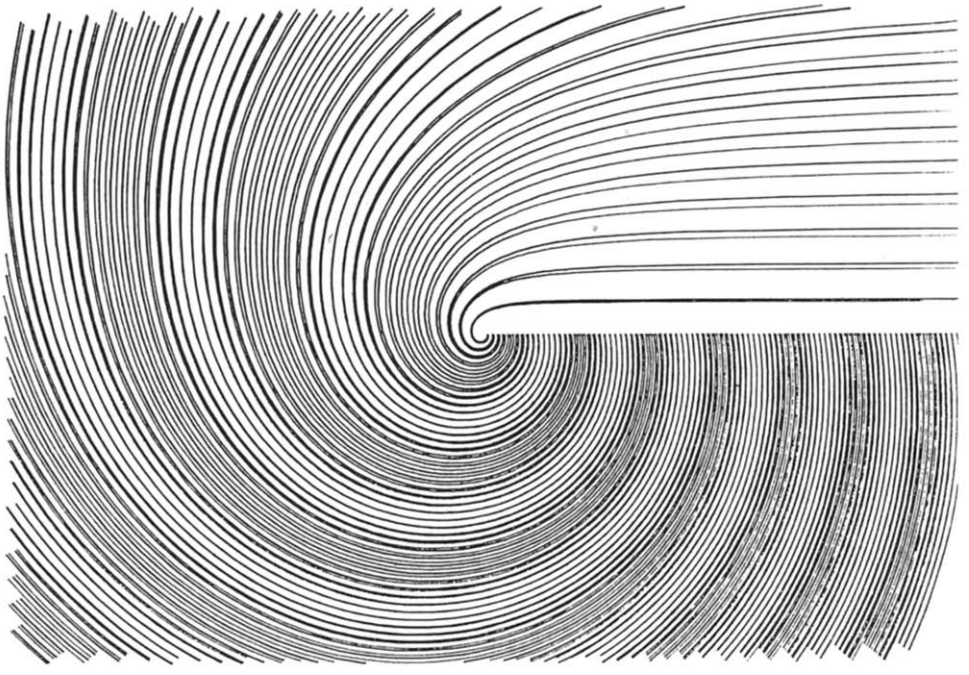

Fig. 27.

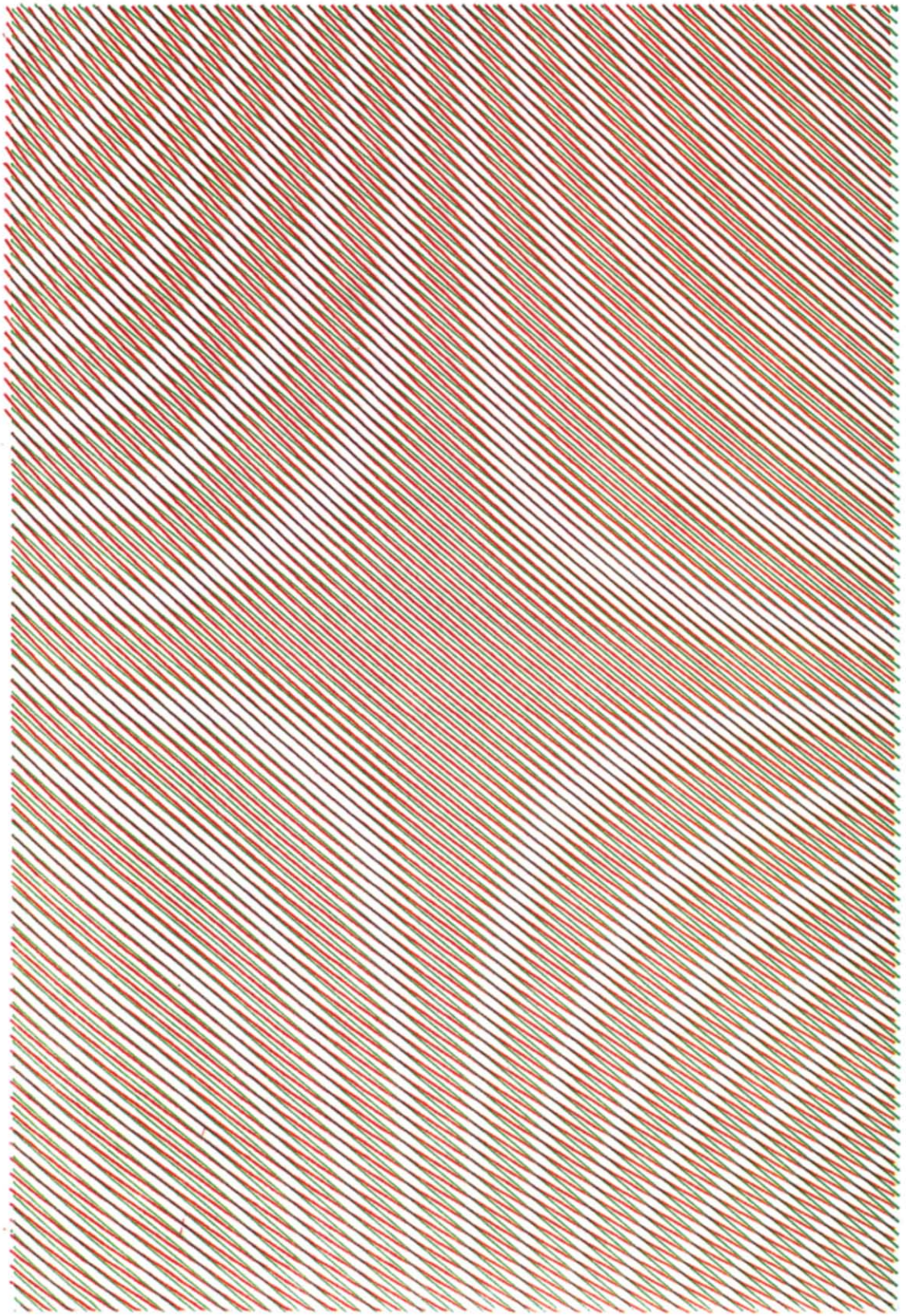

Fig. 28.

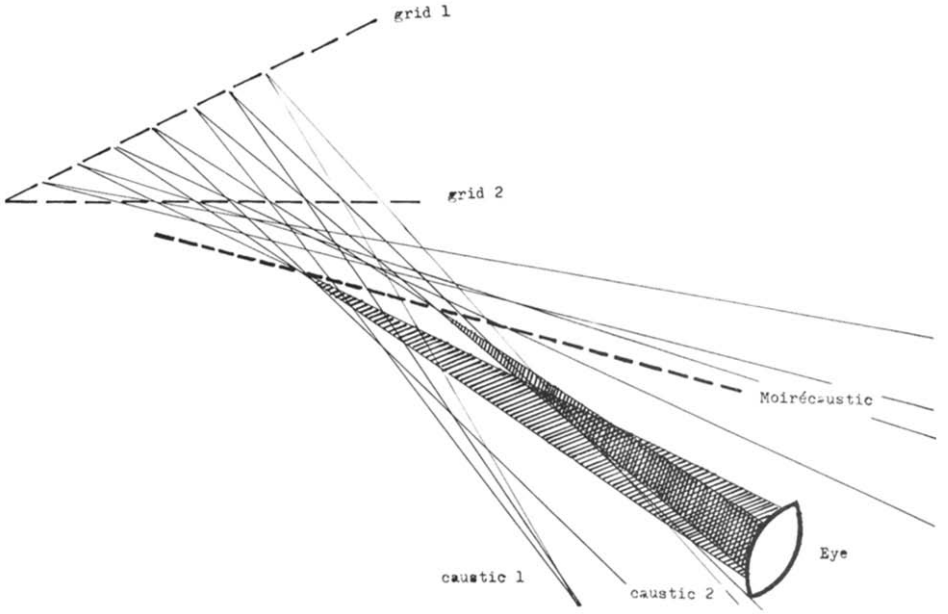

Fig. 29.

that can be observed on real Moiré objects. Two interpretations of spatial Moiré are proposed in this section.

The first interpretation explains spatial Moiré locally as a plane Moiré. If the two systems of discrete lines, the u- and v-lines, on the graphs of two functions are projected from a center, the eye of the observer, onto a reference plane, that may be the background of the eye, a spatial Moiré results. The Figs. 30(a), 31(a) show spatial Moirés constructed according to this interpretation. The designed axes of the system of coordinates indicate the direction of the line of

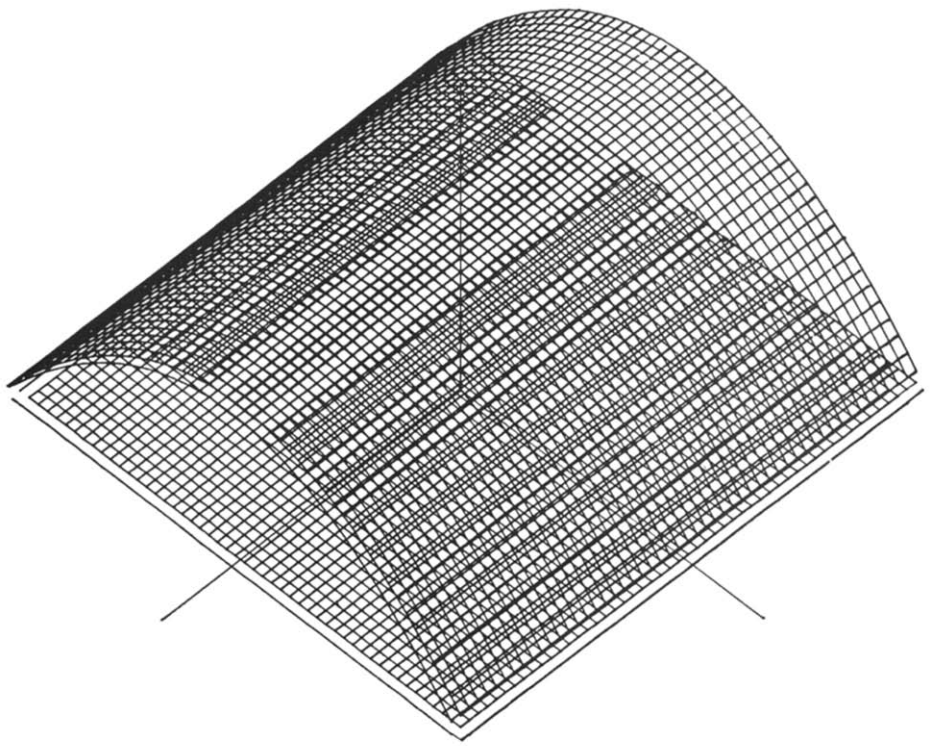

a

Fig. 30(a–c).

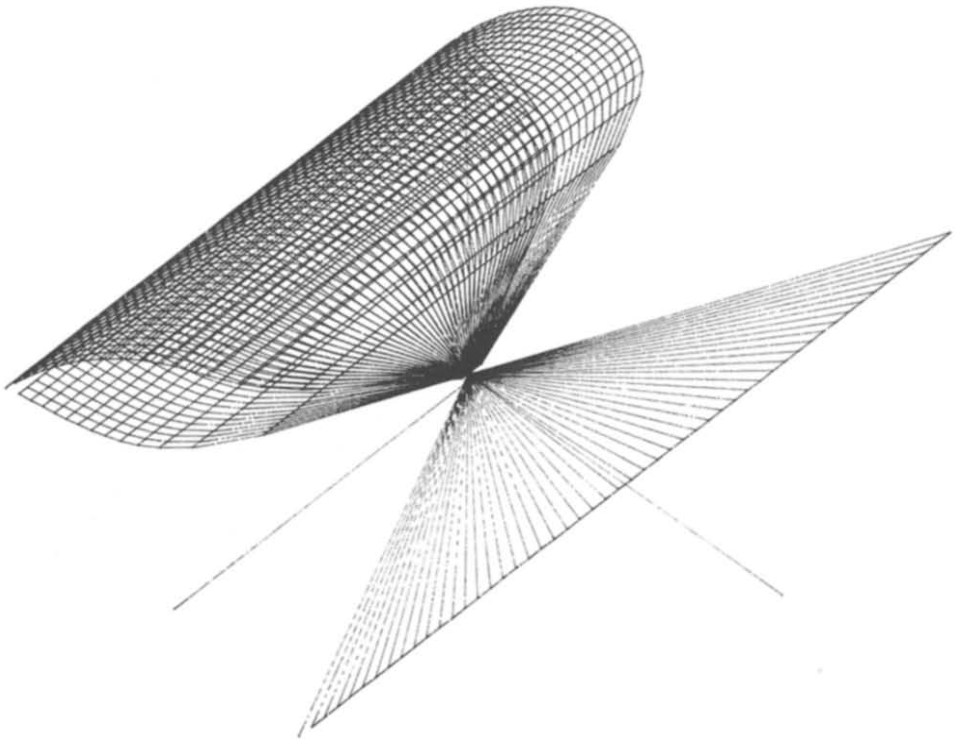

b

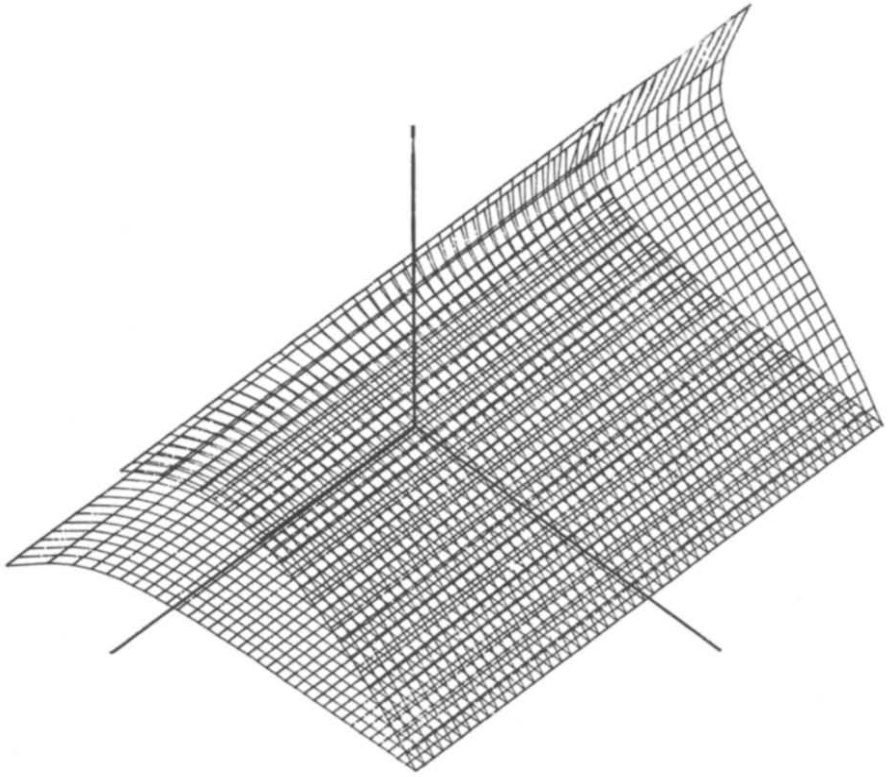

c

Fig. 30. (*Con't*)

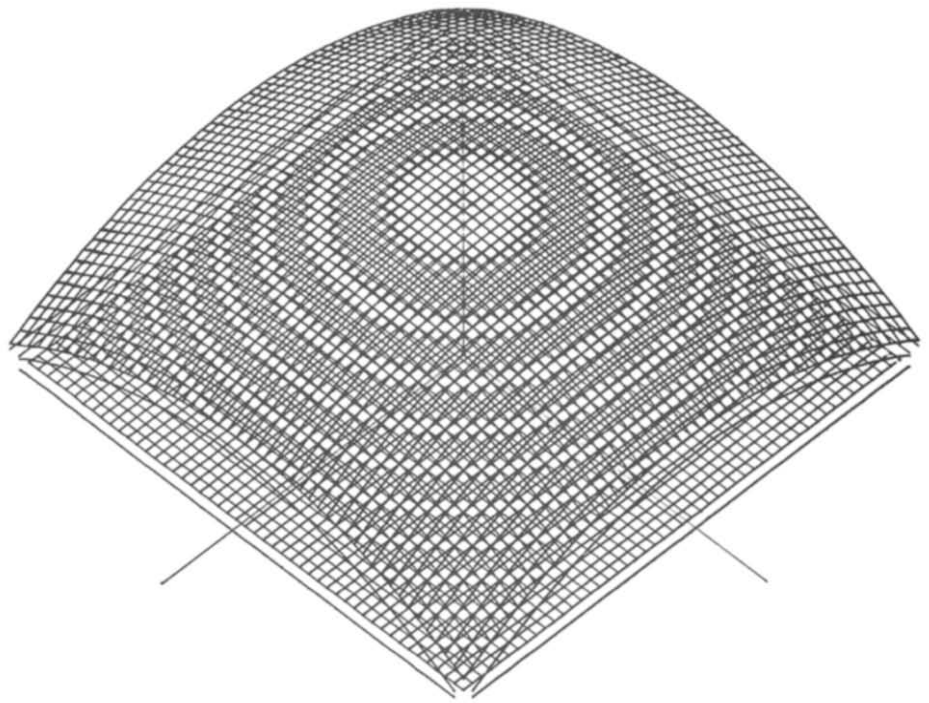

a

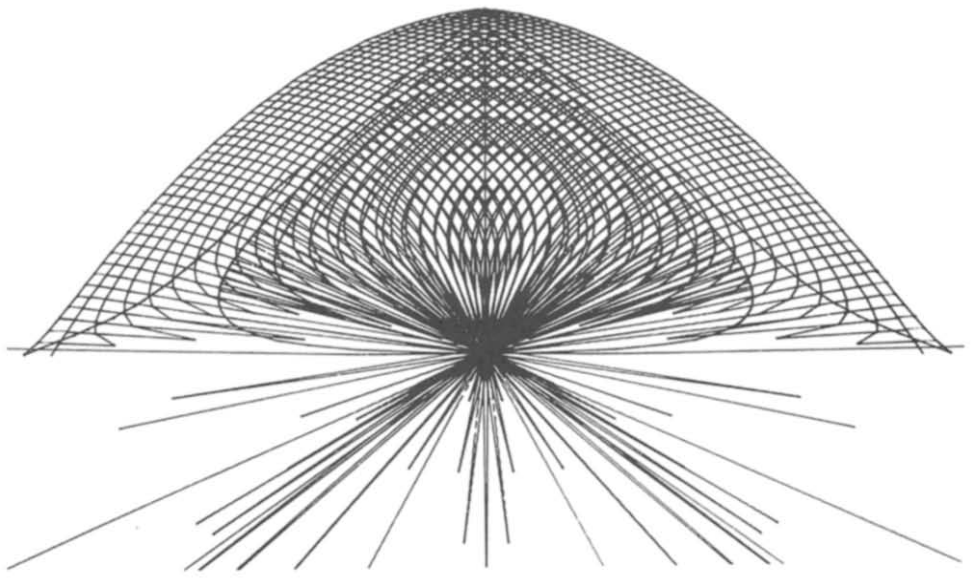

b

Fig. 31(a–d).

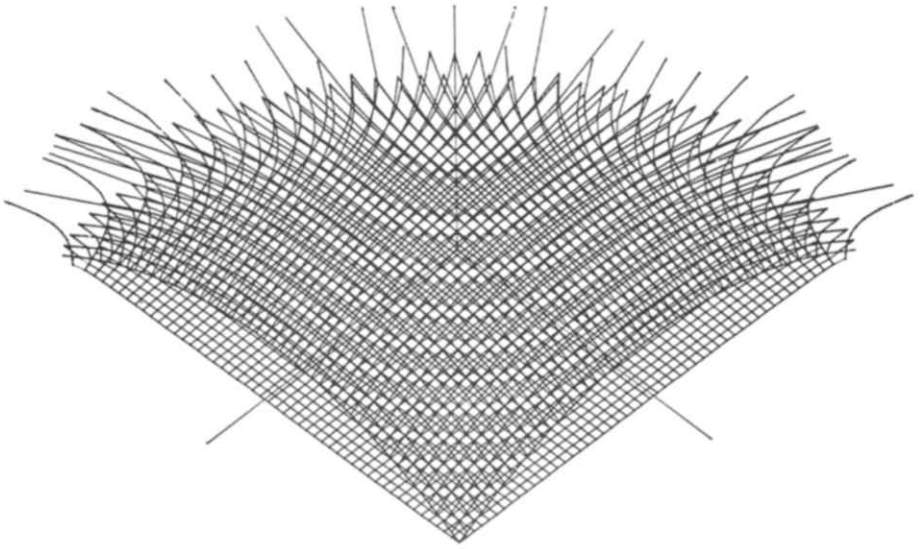

c

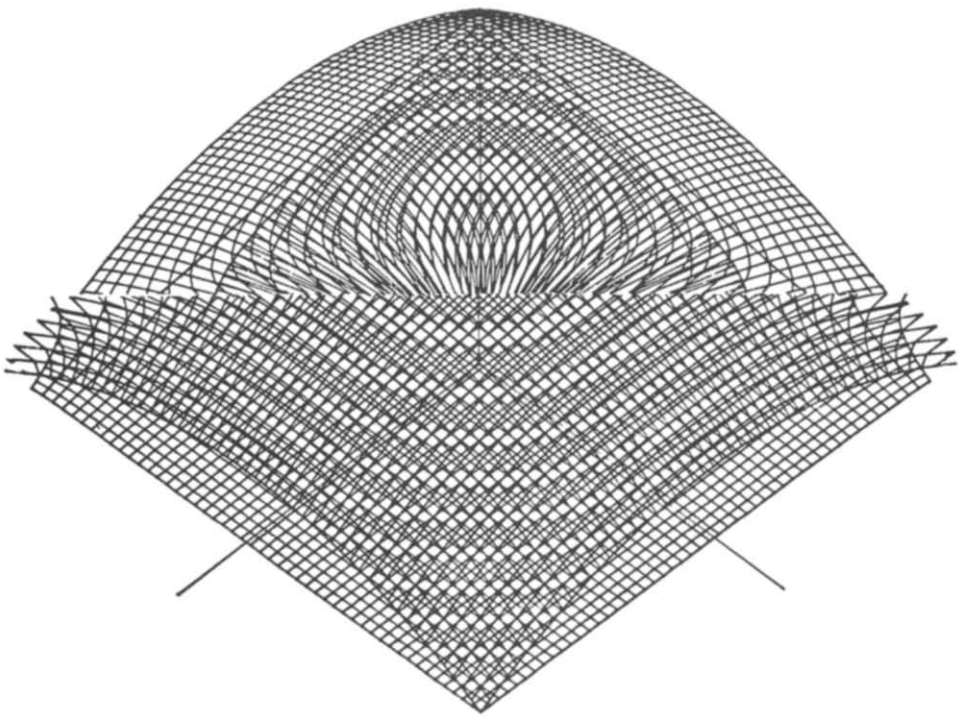

d

Fig. 31. (*Con't*)

sight. It must be mentioned that little changes in the positions of the causing screens have dramatic effects in the Moiré.

The second interpretation was given by Theocaris *et al.*[4] and will be described in Appendix 2 in a modified way which is elementary, computer-adapted and does not use line geometry[5]. This interpretation answers the question where the spatial Moiré is located.

Figure 29 explains the construction of the locus of spatial Moiré for the most simple situation. Corresponding lightrays through the holes of the plane screens or grids shown in profile define the different caustics. The eye of the observer sees a lightpoint in the real or virtual point of intersection of lightrays entering the eye. In the given situation the different Moiré-lines which are perpendicular to the plane of the Fig. 29 seen by the observer too lie on a plane, the Moiré-caustic.

We term the spatial Moiré *real* if the Moiré-caustic is in front of, *virtual* if it is behind the causing screens relative to the observer.

If the nets of lines on z_1 and z_2 of Figs. 30(a) and 31(a) are mapped onto the Moiré-caustic we obtain Fig. 30(b, c) and Fig. 31(b, c). Figure 31 (b) gives real, Fig. 31(c) virtual Moiré-caustic. It should be noted that the two Moirés of Figure 31(b) and 31(c) must be combined additively, i.e. white and black gives white. This combination is shown for Figs. 31(b) and 31(c) in 31(d). The resulting pattern differs greatly from Fig. 31(a) and demonstrates the difficulties in interpreting spatial Moirés.

REFERENCES

1. G. Oster and Y. Nishijima, Moiré patterns. *Scientific American* **208** (1963).
2. J. Walker, Visual illusions in random-dot patterns and television snow. *Scientific American* **242** (1980).
3. H. Giger, Moirétexturen, in *Catalog of the Kunstmuseum of Berne*, Werner Witschi, Moirés, 5.12.–7.2. 37–44 (1982).
4. P. S. Theocaris, A. P. Vafiadakis, and C. Ziakopoulos, Theory of spatial Moiré fringes, *J. Optical Soc.* Amer. **8**, 1092–1099 (1968).
5. W. Blasdike, Differential Geometrie I, Springer, 261–304, (1929).

APPENDIX 1

THEOREM The Moiré $L_1 \cup L_2$ of two superposed systems L_1 and L_2 of line-fields, each given as the intersection lines of a system of parallel planes with equidistant spacings (the planes not normal to the x-y-plane of the system of coordinates) with the graph of the functions $z_1 = z_1(x, y)$ and $z_2 = z_2(x, y)$ is the contour Moiré of $z = |z_2 - z_1|$. The contours are defined as the middlelines of the Moiré-fringes.

We prove this theorem using the formula of Fig. 19(a) and refering to the symbols explained in this figure.

First suppose that z_1, z_2 are different functions, the graphs of which are planes with normals $\mathbf{N}_i = (a_i, b_i, -1)$ and the equations $z_i = a_i x + b_i y + c_i$, $(i = 1, 2)$. Each of these planes are cut by the parallel and equidistant planes with the normal $\mathbf{N} = (\alpha, \beta, \gamma)$, $\alpha^2 + \beta^2 + \gamma^2 = 1$, $\gamma \neq 0$, whose distance from the origin of the system of coordinates is p, where p denotes an arithmetic series with positive difference Δp. The equation of this system of planes is therefore $E(p)$: $\alpha x + \beta y + \gamma z - p = 0$.

The direction of the intersection lines of $E(p)$ and z_i is given by

$$\mathbf{s}_i = (-\gamma b_i - \beta, \gamma a_i + \alpha, \alpha b_i - \beta a_i), \quad i = 1, 2. \tag{A.1.1}$$

If these vectors are projected onto the x-y-plane we get the vectors $\mathbf{s}_i' = (-\tau_i, \sigma_i)$ with

$$\sigma_i = \gamma a_i + \alpha, \quad \tau_i = \gamma b_i + \beta, \quad i = 1, 2. \tag{A.1.2}$$

The plane $z_i = a_i x + b_i y + c_i$ is cut by $E(p)$ in the straight line $g_i(p)$ whose projection $g_i'(p)$ onto the x-y-plane is given by

$$g_i'(p)\colon [\sigma_i x + \tau_i y - (p - \gamma c_i)]\sqrt{\sigma_i^2 + \tau_i^2} = 0, \quad i = 1, 2. \tag{A.1.3}$$

The distance q_i of $g_i'(p)$ from the origin is therefore given by $q_i = (p - \gamma c_i)/|\mathbf{s}_i'|$. Therefore, the spacing Δq_i of the ruling $g_i'(p)$ is

$$\Delta q_i = \Delta p/|\mathbf{s}_i'|, \quad i = 1, 2. \tag{A.1.4}$$

The angle φ between the two rulings $q_i'(p)$ is determined by the vectors $\mathbf{s}_i'$, $(i = 1, 2)$. Without any restriction of generality we may suppose $\mathbf{s}_i'$ oriented such that $0 < \varphi < = \pi/2$. Therefore, $\cos \varphi = (\mathbf{s}_1' \cdot \mathbf{s}_2')/|\mathbf{s}_1'|/|\mathbf{s}_2'|$. With the formula of Fig. 20 we get

$$d = \Delta p/|\mathbf{s}_2' - \mathbf{s}_1'|. \tag{A.1.5}$$

The vectors $\mathbf{s}_i'$ are related to the vectors $\mathbf{t}_i$ spanning the parallelogram of Fig. 19(a). Because of $|\mathbf{t}_1| = \Delta q_2/\sin \varphi$ and $|\mathbf{t}_2| = \Delta q_1/\sin \varphi$ and $\mathbf{t}_i = \kappa_i \cdot \mathbf{s}_i'$, $(i = 1, 2)$, from $|\mathbf{t}_1 \times \mathbf{t}_2| = \kappa^2 |\mathbf{s}_1' \times \mathbf{s}_2'|$ and $|\mathbf{s}_1' \times \mathbf{s}_2'| = |\gamma||\mathbf{s}_1 \times \mathbf{s}_2|$ we obtain $\kappa = \kappa_1 = \kappa_2 = \Delta p/|\gamma|/|\mathbf{s}_1 \times \mathbf{s}_2|$.

Therefore, with (A.1.4)

$$\mathbf{t}_i = \Delta p \mathbf{s}_i'/|\mathbf{s}_1' \times \mathbf{s}_2'|, \quad i = 1, 2. \tag{A.1.6}$$

According to (A.1.1) and (A.1.2) the vector $\mathbf{s}' = \mathbf{s}_2' - \mathbf{s}_1'$ is given by

$$\mathbf{s}' = \gamma(-b_2 + b_1, a_2 - a_1). \tag{A.1.7}$$

This vector is normal to the vector $\mathbf{M}' = (a_2 - a_1, b_2 - b_1)$ which is the projection of $\mathbf{M} = (a_2 - a_1, b_2 - b_1, -1)$ onto the x-y-plane. But $\mathbf{M}$ is the normal of $z = z_2 - z_1$.

If we set $\mathbf{M} = (a, b, -1)$ with $a = a_2 - a_1$, $b = b_2 - b_1$ for the angle ϵ of the inclination of z we get with (A.1.5) $\tan \epsilon = \sqrt{a^2 + b^2} = |\mathbf{s}'|/|\gamma| = \Delta p/d/|\gamma|$. Therefore, the equidistance H of the contour Moiré of z is

$$H = d \tan \epsilon = \Delta p/|\gamma|. \tag{A.1.8}$$

In the general case where z_1 and z_2 are smooth functions, for each point $P(x, y, 0)$ the tangent planes of z_1 and z_2 have to be cut by planes $E(p)$. In the vicinity of $P(x, y, 0)$, the Moiré of the corresponding line systems L_1 and L_2 is therefore the contourmap of $z = z_2 - z_1$. Because this result is valid for all points $P(x, y, 0)$ the theorem is proven.

It should be mentioned that the planes $E(p)$ can locally be chosen at our discretion if according to (A.1.8) H is taken an constant. If $\mathbf{N}$ is chosen so that it is linearly dependent on $\mathbf{N}_1$ and $\mathbf{N}_2$ the parallelogram of Fig. 19(a) spanned up by the vectors (A.1.6) degenerates. This means that the two rulings are locally parallel to the contours of $z = z_2 - z_1$. This contour Moiré may be called ideal.

APPENDIX 2

A spatial Moiré results in the eye of the observer as union or intersection of two systems of lines or lattices of points, each of which is located on one of the graphs of two functions $z_1 = z_1(x, y)$ and $z_2 = z_2(x, y)$.

Here we describe the spatial Moirés where $z_2 = 0$ and the corresponding lattice of points is given by the points with integer coordinates in the x-y-plane. Each point $A(x, y, 0)$ of this grid shall be mapped on the point $B(x, y, z(x, y))$ of the graph of the function $z_1 = z(x, y)$. The set of these points defines the second lattice. As a realisation we can think of two screens with holes. It is the purpose of the following consideration to show that a spatial Moiré can be interpreted as catastrophe in the sense of Catastrophe Theory.

First we consider the straight lines running through the two points $A(x + a, y + b, 0)$, $B(x, y, z(x, y))$, where a and b are fixed integers. If the line AB is cut by a plane Z = constant, the position of the point of intersection $S(X, Y, Z)$ depends on x and y:

$$\begin{aligned} X &= x + a - aZ/z(x, y) \\ Y &= y + b - bZ/z(x, y). \end{aligned} \tag{A.2.1}$$

The principle of geometric optics—postulating that the eye sees a lightpoint in the real or virtual point of intersection of light-rays entering the eye—suggests the answer to the question of where spatial Moiré is located.

If $A(x(t), y(t), 0)$ is any interpolating curve through the points of the grid in $z_2 = 0$ the point $S(X, Y, Z)$ of (A.2.1) runs through a corresponding line in the plane Z = constant. For those t for which $X(t)$ or $Y(t)$ changes direction an intersection of the corresponding straight lines is realized. Therefore $dX/dt = 0$ and $dY/dt = 0$ are necessary conditions a straight line must fulfill so that in its vicinity such a particular lightray passing the two pointsystems can be found. By differentiating (A.2.1) we get the conditions

$$\begin{aligned} 0 &= \dot{x} + aZ/z^2 \cdot (z_x\dot{x} + z_y\dot{y}) \\ 0 &= \dot{y} + bZ/z^2 \cdot (z_x\dot{x} + z_y\dot{y}), \end{aligned} \tag{A.2.2}$$

where z_x and z_y are the partial derivatives of z.

Now we suppose Z to be chosen in such a way that both of the equations (A.2.2) are fulfilled simultaneously. Eliminating dx/dt and dy/dt in (A.2.2) we get

$$Z/z = -z/(az_x + bz_y) \tag{A.2.3}$$

and therefore, if we write $S(U, V, W)$ for S in this particular position, by substituting (A.2.3) into (A.2.1) we obtain

$$\begin{aligned} U &= x + a + az/(az_x + bz_y) \\ V &= y + b + bz/(az_x + bz_y) \\ W &= -z^2/(az_x + bz_y). \end{aligned} \tag{A.2.4}$$

For each pair (a, b) the set of points $S(U, V, W)$ defines a caustic in the sense of Catastrophe Theory.

If one of the eyes of an observer is at point $E(P, Q, R)$ we select the lightrays that enter the eye and have in their vicinity a tangent of caustic (A.2.4). If $B(x, y, z(x, y))$ is a point of the lattice on the graph of $z_1 = z(x, y)$ and if we join it with the eye by a straight line, the line EB cuts the plane $z_2 = 0$ at a point $A(x_0, y_0, 0)$. Therefore, if we calculate x_0 and y_0 and if in (A.2.4) we set $a = x_0 - x$, $b = y_0 - y$ the point $F(U_1, V_1, W_1)$ on the caustic which corresponds to B is given by

$$\begin{aligned} U_1 &= x - (P - x)z/(R - z) + (P - x)z/((P - x)z_x + (Q - y)z_y) \\ V_1 &= y - (Q - y)z/(R - z) + (Q - y)z/((P - x)z_x + (Q - y)z_y) \\ W_1 &= (R - z)z/((P - x)z_x + (Q - y)z_y). \end{aligned} \tag{A.2.5}$$

Furthermore, if $A(x, y, 0)$ is a point of the grid in $z_2 = 0$, we join it with E by a straight line. This line EA cuts the graph of $z_1 = z(x, y)$ at a point $B(x_0, y_0, x(x_0, y_0))$. If we set $a = x - x_0$, $b = y - y_0$ we obtain the following system of equations for a and b:

$$a/(P - x) = -z(x - a, y - b)/R = b/(Q - y). \tag{A.2.6}$$

Therefore, if we replace x by $x_0 = x - a$ and y by $y_0 = y - b$ in z, z_x, z_y from (A.2.5) we get the point $G(U_2, V_2, W_2)$ on the caustic which corresponds to $A(x, y, 0)$ in $z_2 = 0$.

It's obvious that the points F and G lie on the same graph which we shall name Moiré-caustic. F and G are the pictures of the corresponding points B and A of the lattice in $z_1 = z(x, y)$ and of the grid in $z_2 = 0$. Therefore, the two systems (A.2.5) and (A.2.6) can be mapped onto the Moiré-caustic, where they produce the spatial Moiré that may be seen by the eye at E.

If we specify $z_1 = mx$, the two mappings can be explicitly calculated. If the observer is far away from the observable piece of Moiré-caustic the observed Moiré is a plane. This result is given in[4]. It can easily be obtained by specializing (A.2.5) and (A.2.6). If we set $\lambda = P/R$ and $\mu = Q/R = 0$, for R tending to infinity, we obtain the following mappings of the two point systems on the Moiré-caustic:

$$\begin{aligned} U_1 &= (2 - \lambda m)x \\ V_1 &= y \\ W_1 &= x/\lambda. \end{aligned} \tag{A.2.7}$$

$$\begin{aligned} U_2 &= (2 - \lambda m)x/(1 - \lambda m) \\ V_2 &= y \\ W_2 &= x/\lambda. \end{aligned} \tag{A.2.8}$$

By eliminating x from (A.2.7) and (A.2.8) we get the function whose graph is the Moiré-caustic

$$W = U/\lambda/(2 - \lambda m). \tag{A.2.9}$$

The formula also can be obtained with the methods of line geometry [5]. Discussion of (A.2.9) substantiates the following rule: If the two plane grids form a wedge and if from the side of its edge the spatial Moiré is seen, the Moiré-caustic is virtual. If the Moiré is seen from the opposite side and the eye E is not enclosed by the two planes of the grids, the Moiré-caustic is real. The difference in the observation can easily be tested if the wedge is laid with one side on a white background. Figures 30(b, c) and 31(b, c) are constructed with (A.2.5) and (A.2.6).